Acta Pharmaceutica Sinica B 2026;16(6):3655−3679

Chinese Pharmaceutical Association
Institute of Materia Medica, Chinese Academy of Medical Sciences

Acta Pharmaceutica Sinica B

www.elsevier.com/locate/apsb
www.sciencedirect.com

ORIGINAL ARTICLE

Steroid hormone ouabain cooperates with Na^+, K^+-ATPase to improve innate immunity against bacterial infections through a non-classic training mechanism regulated by mRNA reprogramming

Lili Chen[a,†], Kuida Chen[a,b,†], RunRun Shan[a,†], Jinjun Bian[c], PeiPei Jin[c], Hao Lin[a], Jian Liu[a], Yan Chen[a], Siyao Zhu[d], Fangzhou Yin[e,*], Wu Yin[a,*]

[a]*State Key Lab of Pharmaceutical Biotechnology, College of Life Sciences, Nanjing University, Nanjing 210023, China*
[b]*Department of Intensive Care Unit, Northern Jiangsu People's Hospital, Yangzhou 225001, China*
[c]*Faculty of Anesthesiology, Changhai Hospital, Naval Medical University, Shanghai 200433, China*
[d]*Harvard T.H. Chan School of Public Health, Boston, MA 02115, USA*
[e]*School of Pharmacy, Nanjing University of Chinese Medicine, Nanjing 210023, China*

Received 29 July 2025; received in revised form 18 September 2025; accepted 7 October 2025

KEY WORDS

Innate immune cells;
Immune training;
mRNA reprogramming;
Endotoxin tolerance;
Posttranscriptional RNA regulons;
Steroid hormone ouabain;
Na^+,K^+-ATPase;
CYTOR

Abstract Epigenetic reprogramming underpins trained immunity (TRIM). However, the importance of mRNA reprogramming in TRIM remains unknown. Here, we discovered, for the first time, that the steroid hormone ouabain creates a significant training effect on peripheral innate immune cells (IICs), leading to functional enhancement of IICs against bacterial infections. However, unlike conventional training mechanisms, ouabain primarily relies on an integrated posttranscriptional RNA regulon complex (IPRRC) to establish immune memory and reprogram cytokine expression, with lncRNA-CYTOR playing a critical role in this process. Moreover, to enhance training effects while reducing lactate production, ouabain promotes a rapid degradation of the Na^+,K^+-ATPase receptor. Pathologically, endogenous ouabain is downregulated in sepsis-induced immunoparalysis *in vivo*, correlating with impaired innate immunity. Exogenous ouabain rescue significantly reverses this impairment, and its effect is superior

*Corresponding authors.
E-mail addresses: wyin@nju.edu.cn (Wu Yin), yinfangzhou@njucm.edu.cn (Fangzhou Yin).
†These authors made equal contributions to this work.

Peer review under the responsibility of Chinese Pharmaceutical Association and Institute of Materia Medica, Chinese Academy of Medical Sciences.

https://doi.org/10.1016/j.apsb.2025.12.041

to β-glucan, even when used at one percent of β-glucan dosage. Notably, posttranscriptional RNA regulons are also critically involved in β-glucan's training effects. Overall, mRNA reprogramming emerges as a new mechanism for TRIM; steroid hormone ouabain is a novel innate immunity regulator.

1. Introduction

Sepsis is a life-threatening condition characterized by a dysregulated body's response to infection[1], often associated with profound immune disorders[2,3]. As the global population continues to age and the spread of highly pathogenic microorganisms increases, the incidence and mortality rates of sepsis are expected to rise significantly in the future. This trend poses significant threats to human health and will result in substantial social and economic burdens.

During sepsis, two opposing immune states occur: hyperinflammation followed by immunoparalysis[2,4,5]. Immunoparalysis significantly contributes to the high mortality rate associated with sepsis, yet effective clinical treatments are lacking[2,5,6]. Immunoparalysis involves various pathological changes, with impairment of innate immunity being crucial, as it serves as the first line of defense against pathogen invasion[3]. During immunoparalysis, innate immune cells (IICs) show reduced responsiveness to bacterial infections, exhibiting a phenotype akin to endotoxin tolerance[7,8]. A prompt reversal of this tolerant state is crucial to prevent the further progression of sepsis[9,10]. Another key characteristic of immunoparalysis is widespread metabolic defects in IICs[11]. The tolerant IICs can lead to a significant loss of metabolic plasticity[12], and lactate production plays a crucial role[13]. Addressing both the immune and metabolic disorders of IICs is therefore critical for effectively intervening in immunoparalysis.

Endocrine hormones play essential roles in regulating immune and metabolic balance during sepsis, with cortisol being the primary treatment approach in clinical settings aimed at restoring this balance[14]. Cortisol shares a precursor and a similar core structure with the steroid hormone ouabain[15]. Ouabain can significantly enhance recovery from sepsis-induced immunoparalysis by acting as an immunostimulant[16]. But paradoxically, ouabain also demonstrates a protective effect in sepsis models characterized by hyperinflammation[17]. Why ouabain benefits these two opposing immune states in sepsis remains elusive.

Ouabain is a naturally occurring compound that helps defend against threats[15,18]. Following the discovery of Na^+,K^+-ATPase (NKA), it became evident that ouabain is a natural ligand of this enzyme. NKA is a membrane-bound ion transporter responsible for moving sodium (Na^+) and potassium (K^+) ions across the cell membrane against their electrochemical gradients. This process consumes a substantial portion of a cell's ATP supply, accounting for one-half to one-third of cellular ATP expenditure. Consequently, NKA is one of the largest consumers of ATP in mammals, and its function closely couples with the glycolysis process[19] and energy metabolism[20]. NKA is primarily composed of α and β subunits, with the predominant isoforms found in immune cells being $\alpha1\beta1$, in which $\alpha1$ serves as the catalytic subunit. When ouabain binds to NKA in cardiac cells, it reduces cellular ATP consumption, resulting in significant cardioprotective effects[21]. Ouabain has been developed into a clinically effective drug for treating heart diseases in Europe, and it is considered the "insulin of the heart"[22]. Interestingly, ouabain is also present in the serum of mammals, where it is referred to as endogenous ouabain (EO). EO is a hormone-like substance primarily produced by the adrenal glands using cholesterol as a precursor[23]. The concentration of EO in serum is relatively low, ranging from picograms to low nanograms per milliliter. Increasing evidence suggests that EO does not significantly inhibit the ion transport activity of NKA. Instead, it utilizes NKA as a scaffold protein to organize protein complexes and facilitate signaling events, such as Src activation[18]. Due to this property, EO/NKA-mediated signaling is implicated in various pathophysiological processes. However, its role in sepsis immunity remains unknown.

While ouabain has demonstrated effectiveness in improving sepsis immunity, several important issues remain yet unsolved. First, the role of NKA in the immunomodulatory effects of ouabain during sepsis is not well understood. Second, the role of EO in regulating immunity during sepsis, particularly in the context of immunoparalysis, remains unclear. Third and most importantly, ouabain has a rapid metabolic clearance rate *in vivo*, with a plasma half-life of less than 10 min[24]. This fact raises questions about how the brief duration of ouabain's signaling can result in a lasting effect *in vivo*.

To address those concerns, our study demonstrates that ouabain can exert a training effect on peripheral IICs. This property enables the IICs to remember the effects of ouabain, resulting in an enhanced response to a subsequent LPS stimulus *in vitro* or during bacterial infections *in vivo*. Trained immunity (TRIM) is a crucial adaptive mechanism that enables the host's immune system to respond effectively to external stimuli[25]. The microbial product β-glucan is a well-established TRIM inducer[26]. Induction of TRIM is effective against immunoparalysis in sepsis models[27,28]. Ouabain demonstrated a significant training effect on IICs, particularly when they are in a state of tolerance. However, unlike traditional training methods that involve epigenetic reprogramming[28,29], ouabain trains cells through mRNA reprogramming. It achieves this by rapidly increasing the production of lncRNA-CYTOR, CYTOR then collaborates with other RNA regulons and relevant signaling molecules to form an integrated posttranscriptional RNA regulon complex (IPRRC). This IPRRC-mediated mRNA reprogramming not only enables ouabain to quickly enhance the function of IICs against bacterial infections, but it also supports the memory of this effect for an extended period. Moreover, to enhance the training effects while reducing lactate production, ouabain even

promotes a rapid degradation of NKA α1 in IICs. Pathologically, serum EO levels are significantly downregulated in immunoparalysis, correlating with a reduction in innate immunity against bacterial infections. Exogenous ouabain rescue can effectively reverse this impairment, and its effect is superior to β-glucan. Importantly, posttranscriptional RNA regulons are also involved in β-glucan-mediated training effect. In summary, mRNA reprogramming emerges as a new mechanism for TRIM; the steroid hormone ouabain is identified as a novel TRIM inducer and innate immunity regulator.

2. Materials and methods

2.1. Cell lines and animals

Human monocyte cell line (THP-1), murine macrophage cell line (RAW 264.7), human embryonic kidney cells (HEK 293T), and type II lung epithelial cells (A549) were purchased from the American Type Culture Collection (ATCC; Manassas, VA, USA). THP-1 cells, RAW 264.7 cells, and A549 cells were cultured in RPMI 1640 medium (Wisent, Canada) containing 10% fetal bovine serum (Thermo Scientific, USA) and penicillin (100 U/mL)/streptomycin (100 μg/mL) (Wisent, Canada). HEK293T cells were cultured in DMEM (Wisent, Canada) supplemented with 10% FBS and penicillin (100 U/mL)/streptomycin (100 μg/mL). All cells were maintained in a humidified atmosphere at 37 °C with 5% CO_2.

2.2. Animals

The male C57BL/6 mice, aged 6−8 weeks, were purchased from the Model Animal Research Center at Nanjing University in Nanjing, China. The heterozygous Na^+,K^+-ATPase α1 $(NKA\alpha1)^{+/-}$ mice were obtained from the Shanghai Model Animal Center of China. The C57BL/6JGpt-MORRBID^{em1Cd195480}/Gpt mice were supplied by GemPharmatech Co., Ltd. in Nanjing, China. All animal experiments were conducted following protocols approved by the Ethics Committee of Nanjing University (IACUC-D2210004) and adhered to the Guide for the Care and Use of Laboratory Animals established by the National Institutes of Health, USA.

2.3. Clinical sample collection

Patients with sepsis was enrolled in this study from the Intensive Care Units (ICU) (Department of Anesthesia, Shanghai Changhai Hospital, Affiliated Hospital of the Second Military Medical University) during the years 2011−2013[30]. This study also includes HDs for comparison. All participants conformed to the criteria established by the 2001 SCCM/ESICM/ACCP/ATS/SIS International Sepsis Definitions Conference[31]. The Shanghai Changhai Hospital Ethics Committee approved the experiments of human subjects. All patients involved in this project provided informed consent, and the experiments conformed to the principles outlined in the WMA Declaration of Helsinki and the Department of Health and Human Services Belmont Report. This part of the study was registered with Clinicaltrial.gov under NCT01976884. The sepsis patients enter a state of immunoparalysis, as indicated by a low level of mHLA-DR expression (<30%) on $CD14^+$ monocytes[10].

2.4. Reagents and antibodies

Ouabain octahydrate (purity 99%, HY-B0542), β-D-glucan (HY-139413), anti-mouse PD-L1 Ab (HY-P99145), protein A/G magnetic beads (HY-K0202), streptavidin magnetic beads (HY-K0208), Gö 6983 (HY-13689), GSK-3β inhibitor 1 (HY-126144), SB203580 (HY-10256), BAY11-7082 (HY-13453), and erlotinib (HY-50896) were all purchased from MedChemExpress (NJ, USA). ActD (SBR00013) and LPS (L2880) were obtained from Sigma−Aldrich (Saint Louis, MO, USA). Lipofectamine 2000 was obtained from Invitrogen (CA, USA). Polyjet (SL100688) transfection reagent was purchased from SignaGen (Gaithersburg, MD, USA). Antibodies against c-Fos and c-Jun were purchased from Cell Signaling Technology (Beverly, MA, USA). Monoclonal antibodies against HuR and the cleaved caspase-3 (ab2302) were obtained from Abcam (Cambridge, UK). The Myc-tag and PKCα antibodies were purchased from ZenBio Co. (Chengdu, China). Antibodies against p-EGFR (Y1045) were from Abclonal (Wuhan, China). Primary antibodies against p-EGFR (Y1068), FLAG-tag (DDDDK-tag), GAPDH, HA-tag, lamin B1, p-PKCα, PKCδ, tubulin, and secondary antibodies, including goat anti-rabbit IgG, goat anti-rabbit IgG-HRP, and goat anti-mouse IgG-HRP were all obtained from Bioworld (Nanjing, China).

2.5. Preparation of polyclonal antibody against ouabain

A 6-week-old female Japanese white rabbit was immunized subcutaneously five times with ovalbumin-conjugated ouabain (Shunkang Biotech. Co., Hubei, China). A boosting immunization was conducted a week after the third immunization. The dose of antigen for each immunization was 300−600 μg. Freund's complete and incomplete adjuvants (Sigma−Aldrich, Shanghai, China) were used in the first and last four immunizations. At 75 days after immunization, the rabbit was sacrificed, and the serum containing anti-ouabain polyclonal antibodies was separated. A series of antibody dilutions were then loaded onto 96-well plates pre-coated with ouabain-BSA to examine antibody reactivity. Then, the antibodies were subjected to column purification, and their purity was analyzed using SDS-PAGE analysis. The purified antibody was diluted to test its specificity for ouabain and to assess its lack of cross-reactivity with other cardiac steroids, such as digoxin.

2.6. Plasmid construction

To construct the human TNF 3′-UTR luciferase reporter plasmid, the 3′-UTR fragment of TNF was cloned into the a pGL3-Basic vector downstream of the firefly luciferase reporter gene (Madison, WI, USA). To construct a luciferase reporter driven by CYTOR promoter variants, the full-length CYTOR promoter and its deletion mutants were amplified by PCR and cloned into pGL3-Basic vector *via* Kpn I and Xho I cloning sites. To map the HuR domain for CYTOR binding, deletion mutants of HuR (ΔRRM1, ΔRRM2, and ΔRRM3) and HuR-RRM3 alone were amplified by PCR and cloned into FLAG-tagged pRK5 mammalian expression vector. Their expressions were confirmed by Western blot analysis. HuR mutants with serine 221 and 158 mutations changed to alanine were generated using the PCR site mutagenesis method. To map CYTOR nucleotides for HuR binding, deletion mutants of CYTOR (1−48 nt, 1−85 nt, 49−85 nt, 86−255 nt, and 256−542 nt) were amplified by PCR,

and their expressions were examined by agarose gel electrophoresis. To identify the nucleotides in the 1−48 nt loop structure of CYTOR for HuR binding, two mutations were introduced into the loop structure of CYTOR by PCR site mutagenesis. The coding sequence (CDS) of human EGFR was cloned into the FLAG-tagged pRK5 expression vector. The CDS of PKCα and Grb2 were inserted into the MYC-tagged pCMV expression vector. The CDS of c-Cbl was cloned into the HA-tagged pRK5 expression vector. The complete RNA sequence of CYTOR (transcript variant 3) and MORRBID (transcript variant 3) were amplified by PCR and inserted into the pcDNA3.1 vector to create their overexpression plasmids. The CYTOR-mut-1 plasmid harbors mutations in the 1−48 nt loop structure, failing to bind HuR. The CYTOR-mut-2 plasmid harbors mutations that lead to failure in TNF 3′-UTR binding. The CYTOR-mut-3 plasmid harbors mutations that lead to failure in miR-181d-3p binding. All primer pairs are provided in the Supporting Information Table S1.

2.7. CLP polymicrobial sepsis model

Following the previously described procedures[16,32-34], male C57BL/6 mice, aged 6 to 8 weeks, were anesthetized with an intraperitoneal injection of 0.3% pentobarbital sodium. A 1 cm midline incision was made in the ventral surface of the abdomen. The cecum was exteriorized, and approximately 50% of the distal end was ligated with a 3-0 silk suture and punctured with a 20-gauge needle. In a sham group, a laparotomy was performed in which the cecum was manipulated but neither ligated nor punctured. A single dose of imipenem (25 mg/kg) was administered subcutaneously 1 h after CLP surgery. The control group, consisting of sham-operated mice, received the same treatment as the experimental group. One day after the CLP procedure, all animals received 1 mL of 0.9% saline subcutaneously. Bacterial infections, introduced as a secondary insult, occurred at 48 or 72 h after CLP surgery. CLP mice were injected intraperitoneally with 2×10^3 *Salmonella enterica* Serovar *typhimurium (S.tm.)* or 1×10^6 *Pseudomonas aeruginosa pneumonia (PA)* in 100 μL. Forty-eight hours after the CLP surgery, there was a significant decrease in the production of serum TNF, IL-6, IL-1β, and IFN-γ. In contrast, the production of IL-10 increased, along with higher bacterial loads in both the blood and spleen. Additionally, there was a development of macrophage tolerance to LPS and increased apoptosis of $CD4^+$ and $CD8^+$ T cells in the spleen. This state is referred to as immunoparalysis[9,32]. Furthermore, a secondary bacterial infection occurring at 48 or 72 h post-CLP exacerbates immunosuppression and results in a higher mortality rate among the animals.

2.8. CLP mice with bilateral adrenal gland removal

The surgical removal of adrenal glands from mice was performed as previously described with minor modifications[35]. Male C57BL/6J mice (6 to 8 weeks old) were anesthetized with isoflurane and disinfected with iodophors. After the kidneys were exposed by surgery, bilateral adrenal glands were bluntly separated and removed after ligation. Both muscles and skin were sequentially sewn and sterilized with iodophors. After regaining consciousness, the mice were returned to a squirrel cage and provided food and water *ad libitum*. Mice in the sham group received the same surgery except for bilateral adrenal gland removal. CLP surgery was performed on these adrenal-null mice 2 weeks later.

2.9. CLP mice with macrophage depletion and reconstitution

C57BL/6 mice underwent macrophage depletion using clodronate-containing liposomes and macrophage reconstitution *via* the adoptive transfer of BMDM cells, following previously described procedures[36]. In brief, 200 μL clodronate liposome was injected (i.p.) twice into mice at 2 and 4 days before CLP surgery. At 48, 72, 96, and 128 h after CLP, mice were injected with ouabain-trained BMDM cells (10^6 per mouse) *via* the tail vein. In this experiment, a secondary PA infection was introduced at 72 h after CLP surgery. Following the experiments, bacterial loads in peritoneal lavage fluid and organs, including the kidney, spleen, liver, and lungs, were quantified. Serum TNF, IL-6, and lactate production were also measured.

2.10. Isolation of human $CD14^+$ monocytes

The preparation of human peripheral blood mononuclear cells (PBMC) was performed as described previously[16]. In brief, blood cells were harvested from the interphase layer after centrifugation of heparinized blood, washed three times in PBS, and the pellets were resuspended in RPMI 1640 medium supplemented with 10% FBS, 100 U/mL penicillin, and 100 μg/mL streptomycin. After overnight incubation, the non-adherent cells were removed, and the remaining adherent cells were identified as PBMCs. To isolate $CD14^+$ monocytes, the pool of PBMCs was incubated with Dynabeads CD14 (No. 11149D, Invitrogen, USA); $CD14^+$ monocytes were then positively selected by magnet sorting, following the manufacturer's procedures.

2.11. Analysis of single-cell RNA sequencing

The single-cell RNA-Seq data set (GSE167363)[37] was analyzed using the Seurat package, and the UMAP (Uniform Manifold Approximation and Projection) method was employed to visualize the cell clusters of PBMCs (Peripheral Blood Mononuclear Cells) extracted from healthy controls and patients with sepsis. The determination of cell types was based on the expression of cluster gene markers. The DESeq2 package in the R language was used to determine the difference in CYTOR expression in human monocytes.

2.12. Microarray analysis of human PBMCs

PBMCs collected from patients with sepsis-induced immunoparalysis were treated with ouabain at a concentration of 100 nmol/L for 12 h. After treatment, total cellular RNA was extracted using TRIzol and hybridized with an Affymetrix® GeneChip (Human Gene 1.0 ST array). With whole-transcript expression analysis, lncRNAs significantly upregulated by ouabain were selected for further study.

2.13. Determination of serum endogenous ouabain content

Serum EO levels in humans and mice were determined using an ELISA kit according to the manufacturer's instructions[35] (JL19863, JL46606, Jianglai Biotech. Co., Shanghai, China). In brief, the heparinized blood samples were centrifuged, and the supernatant was subject to serum EO measurement. The standard curve was established by measuring the optical density (OD) of

standard solutions at concentrations of 2.5, 5, 10, 20, 40, and 80 pg/mL at a wavelength of 450 nm. Then, the serum EO in each specimen was detected using a double-antibody sandwich enzyme-linked immunosorbent assay (ELISA). The supernatant of the samples and horseradish peroxidase (HRP)-labeled detection antibodies were sequentially added to the wells that were pre-coated with human ouabain capture antibodies. HRP converted the substrate TMB to a yellow compound. The serum EO content was determined by measuring the OD at 450 nm and calculating it according to the standard curve.

2.14. Isolation of mouse PBMCs, peritoneal macrophages, and BMDMs

The method for preparing mouse PBMCs was similar to that for human PBMCs. Peritoneal macrophages were collected by injecting 5 mL cold PBS into the peritoneal cavity of euthanized mice, followed by gentle abdominal massage and fluid retrieval. The cells were centrifuged, resuspended in RPMI-1640, and counted for further use. The cell's purity was examined by flow cytometry using F4/80 and CD11b markers. BMDMs were isolated from 8 to 12-week-old C57BL/6 mice by flushing femurs and tibias with PBS. After red blood cell lysis, the cells were resuspended in RPMI1640 medium with 10% FBS, 2 mmol/L L-glutamine, and 20 ng/mL M-CSF and plated at 1×10^6 cells/mL. Cells were cultured at 37 °C with 5% CO_2 for 7 days, with medium changes every 3 days. On Day 7, the adherent macrophages were harvested.

2.15. Establishment of HuR knockout macrophages

CRISPR/cas9 technology was used to produce *HuR* gene knockout RAW264.7 cells. The single-guide (sg) RNAs for Cas9 nuclease targeting *HuR* in the mouse genome were provided by Invitrogen (TrueGuide™ Synthetic sgRNA, Thermo Fisher Scientific, China). The 20-nt target sequences in the exon 4 of *HuR* (*HuR* sgRNA sequence, 5′- ATATGCTCGCCCAAGCTCAG-3′), including the protospacer adjacent motif (PAM; 5′-AGG-3′), were selected for their predicted high score and reduced off-target effects. After transfection with PX459 plasmid expressing Cas9 (Addgene) and optimized sgRNAs and transient selection with puromycin (Invitrogen), cells were single-cell seeded into 96-well plates without puromycin. To select KO clones, the expression of HuR was determined by Western blot analysis.

2.16. In vitro ouabain training process

Human THP1 cells, human $CD14^+$ monocytes, mouse RAW264.7 cells, and mouse BMDMs were treated with ouabain (50 nmol/L) for 24 h at 37 °C. Cells were washed twice with complete DMEM to remove ouabain; complete DMEM was then added, and the cells were further incubated for 5 days. On Day 6, the cells were re-stimulated with LPS (1 μg/mL) for 4 h, and cell responsiveness was examined by measuring TNF mRNA expression. Cells were also stimulated with LPS (1 μg/mL) for 12−24 h, and the cell response was analyzed by measuring TNF production in supernatants using ELISA (BioLegend, 430901).

2.17. In vitro tolerance induction

Human THP1 cells, RAW264.7 cells, BMDMs, and murine peritoneal macrophages were treated with 1 μg/mL LPS for 24 h at 37 °C in a 5% CO_2 incubator. After treatment and PBS wash, the cells were treated with 1 μg/mL LPS for 4 h; TNF mRNA expression in cells or TNF production in the supernatants was measured to examine cell responsiveness.

2.18. Phagocytosis and bacterial clearance assay[38]

For assessing phagocytosis and bacterial clearance, macrophages (PMs or BMDMs) differentiated to maturity were seeded in 24-well plates at a density of 1×10^6 cells/well. Cells were incubated for 24 h to ensure adherence and acclimation to the culture environment. Subsequently, cells were infected with *P. aeruginosa* in its logarithmic growth phase (OD_{600} 0.6−0.8) at a multiplicity of infection (MOI) of 10:1. To measure phagocytosis rate at 15, 30, and 60 min post-infection, supernatants were collected. The percentage of unphagocytosed bacteria in the supernatant was determined by plating serial dilutions on LB agar plates and counting colony-forming units (CFUs). The phagocytosis rate was calculated using Eq. (1):

$$\text{Phagocytosis rate}\ (\%) = 1 - (\text{Total inoculated bacteria (CFU)} / \text{Unphagocytosed bacteria (CFU)} \times 100 \quad (1)$$

To evaluate bacterial clearance rate, cells were treated with 50 μg/mL gentamicin for 1 h to kill extracellular bacteria. At 15, 30, and 60 min post-infection, cells were collected and lysed. The number of viable intracellular bacteria was determined by plating cell lysates on LB agar plates and counting CFUs. The bacterial clearance rate was calculated as Eq. (2):

$$\text{Clearance rate}\ (\%) = 1 - (\text{Initial phagocytosed bacteria (CFU)} / \text{Viable intracellular bacteria (CFU)} \times 100 \quad (2)$$

2.19. Quantification of mRNA, miRNA, and lncRNA expression

According to the manufacturer's instructions, total RNA was extracted from intact cells and tissues using a TRIzol reagent (Sangon Biotech, Shanghai, China). A first-strand cDNA synthesis kit (Yeasen, Shanghai, China) was used to perform reverse transcription. For miRNA, stem-loop qPCR analysis was used as previously described[16]. Real-time quantitative PCR was carried out on ABI StepOne Plus (Applied Biosystems, CA, USA), and the $2^{-\Delta\Delta Ct}$ cycle threshold method was used to calculate the relative expression of RNA. GAPDH was used as an internal control for mRNA and lncRNA, and U6 was used as an internal control for miRNA. Semi-quantitative PCR was performed for 25−32 cycles using gene-specific cDNA primers. All the primers are listed in Supporting Information Table S2.

2.20. Cell transfection with siRNAs and miRNAs

The cholesterol-modified siRNAs against CYTOR, PKCα, PKCδ, MALAT1, UCA1, UCA1, DLEU2, HuR, c-Fos, c-Jun, and cholesterol-modified miRNAs including miR-181d-3p mimics, miR-181d-5p mimics were all synthesized by General Biosystem Co., (Anhui, China). The corresponding siRNA sequences are listed in the Supporting Information Table S3. THP1 cells were transfected with different siRNAs and miRNAs by Lipofectamine 2000. The recombinant plasmids were transfected into HEK293T cells or RAW264.7 cells by Polyjet transfection reagent (Yeasen, Shanghai, China).

2.21. Dual-luciferase reporter assay

Cells were placed at a density of 2×10^5 cells per well; after confluence, cells were co-transfected with a firefly luciferase reporter and *Renilla* luciferase constructs using the Polyjet transfection reagent. The relative luciferase activity in each sample was measured by the Dual-Luciferase® Reporter Assay System (Promega, Madison, WI, USA) following the manufacturer's instructions.

2.22. Measurement of intracellular [Ca^{2+}]

The intracellular [Ca^{2+}] was determined using the fluorescence Ca^{2+} indicator Fluo-4 AM (fluorescent probe, Beyotime, China). Briefly, cells were incubated with Fluo-4 M for 60 min at 37 °C. After washing the cells three times with PBS, the fluorescent signals were quantified using a BD FACScaliber flow cytometer with CellQuest Software (Beckton Dickinson, San Jose, CA, USA), and the results were analyzed with FlowJo VX10 software (TreeStar, USA).

2.23. Measurement of cellular lactate production

Cells after treatment were harvested and resuspended in a cold extraction buffer (1 mL per 5×10^6 cells). The cell suspension was homogenized using an ultrasonic cell disruptor on ice, followed by centrifugation at 12,000 $\times$ *g* for 10 min at 4 °C. The final supernatant was used for lactate measurement using a commercial lactate assay kit (Jiancheng Bioengineering Institute, Nanjing, China; A095-1-1) following the manufacturer's instructions. Absorbance was measured at 570 nm, and lactate concentration was calculated based on a standard curve. Results were normalized to the protein concentration.

2.24. Measurement of cellular ATP content

After treatment, cells were harvested and resuspended in 300−500 μL of cold distilled water. The cell suspension was homogenized on ice and heated in a boiling water bath for 10 min. After vortex for 1 min, the samples were centrifuged at 3500 $\times$ *g* for 10 min. According to the manufacturer's instructions, the supernatant was collected for ATP measurement using a commercial ATP assay kit (Solarbio Life Sciences, Beijing, China; BC2235). Absorbance was measured at 636 nm, and ATP concentration was calculated based on a standard curve. Results were normalized to the protein concentration.

2.25. Western blot analysis

Cells were harvested and lysed on ice with RIPA buffer supplemented with a protease inhibitor cocktail (Beyotime, Shanghai, China). A BCA protein assay kit (Fude Biological Technology, Hangzhou, China) was used to measure the protein concentration. The total protein was separated by SDS-PAGE and transferred to the PVDF membrane. The membrane was blocked with 5% BSA for 1 h at room temperature and incubated with the primary antibody overnight at 4 °C. After washing with PBST, the membrane was incubated with a secondary antibody for 1 h at room temperature. The luminescent substrates were added, and the protein blots were visualized using Tanon image capture software (Beijing, China).

2.26. Protein co-immunoprecipitation assay

After treatment, cells were harvested and lysed, and the total protein was incubated with antibodies overnight at 4 °C. The next day, the mixture was incubated with protein A/G magnetic beads for 2 h at 4 °C. After incubation, the pellets were washed three times with lysis buffer and collected after centrifugation. Western blot assays were used to detect the immunoprecipitated proteins in the pellets.

2.27. EGFR ubiquitination assay

THP1 cells were transfected with siRNA against CYTOR for 36−40 h and then treated with 20 μmol/L MG132 for 6 h before harvesting. Cells were lysed with IP lysate buffer, and after centrifugation, EGFR in the supernatant was immunoprecipitated with rabbit anti-EGFR polyclonal antibody (Proteintech, USA, 18986-1-AP) and protein A/G magnetic beads, and the ubiquitinated form of EGFR was analyzed by Western blot with Ub antibody.

2.28. RNA immunoprecipitation assay (RIP)

RIP assays were performed as described previously[39,40]. Briefly, cells were lysed in RIP lysis buffer (20 mmol/L Tris-HCl, pH 7.5, 100 mmol/L KCl, 5 mmol/L $MgCl_2$, and 0.5% NP-40) on ice for 30 min and then centrifuged at 12,000 $\times$ *g* for 15 min at 4 °C. The supernatants were incubated with antibodies overnight at 4 °C, and then the protein A/G magnetic beads were added for 2 h at 4 °C. The beads were washed with NT2 buffer (50 mmol/L Tris-HCl, pH7.5, 150 mmol/L NaCl, 1 mmol/L $MgCl_2$, and 0.05% NP-40) three times, and the pellets were incubated with 20 units of DNase I for 15 min at 37 °C, further incubated with 0.1% SDS and 0.5 mg/mL Proteinase K for 15 min at 55 °C to remove DNA and proteins. The RNAs in the immunoprecipitation were reverse transcribed and quantified by real-time qPCR analysis.

2.29. Biotinylated RNA pull-down assay

PCR fragments were amplified using forward primers containing the T7 RNA polymerase promoter sequence to obtain the biotinylated transcripts. The primers used are listed in Supporting Information Table S4. After purification of PCR products, the biotinylated transcripts were synthesized using an RNAmax-T7 kit (RiboBio, Guangzhou, China). The whole-cell lysates (500 μg protein per sample) were incubated with 1 μg of the purified biotinylated transcripts for 1 h at room temperature. The addition

of streptavidin magnetic beads and centrifugation precipitated the RNA−protein complex. Western blot analysis was used to detect protein components in the pellets.

2.30. RNA fluorescence in situ hybridization (RNA-FISH)

The Cy3-labeled CYTOR fluorescent probes were synthesized from RiboBio (Guangzhou, China). The RNA-FISH experiments were conducted using the FISH Kit from RiboBio (Guangzhou, China) following the manufacturer's guidelines. In brief, cells were fixed with 4% paraformaldehyde, permeabilized with 0.3% Triton X-100, and then incubated overnight at 37 °C in the dark with specific probes. After hybridization, the process was similar to the indirect immunofluorescence assay. The images were photographed *via* fluorescence microscopy. The probes were designed and provided by the kit supplier.

2.31. Chromatin immunoprecipitation (ChIP) assay

Cells were cross-linked with 1% formaldehyde for 10 min at room temperature, and 0.125 mol/L glycine was used to stop the cross-linking reaction. After the cells were washed with ice-cold PBS three times, the cell pellets were resuspended in ChIP lysis buffer (1% SDS, 10 mmol/L EDTA, 50 mmol/L Tris-HCl, pH 8.1) containing protease inhibitors for 15 min on ice, and then sonicated to shear the genomic DNA. The lysate was centrifuged at 12,000 × *g* for 10 min at 4 °C, and the supernatant was diluted with dilution buffer (0.01% SDS, 1% Triton X-100, 2 mmol/L EDTA, 16.7 mmol/L Tris-HCl, pH 8.1, 150 mmol/L NaCl, and protease inhibitors). The soluble chromatin was incubated overnight at 4 °C with rotation in the presence of anti-c-Fos and c-Jun antibodies, and IgG was used as a negative control. The next day, the chromatin was incubated with protein A magnetic beads for 2 h at 4 °C with rotation. After washing, the protein−DNA cross-linking complex was reversibly cross-linked by incubation overnight at 65 °C and then digested with proteinase K and RNase A. The DNA was isolated from the complex using phenol/chloroform extraction and isoamyl alcohol precipitation. Semi-quantitative PCR analysis detected the binding between chromosomal DNA and c-Fos/c-Jun; the primers are listed in Supporting Information Table S5.

2.32. Indirect immunofluorescence assays

THP-1 cells were fixed in the 4% paraformaldehyde and permeabilized by 0.1% Triton X-100. After washing with PBS, cells were blocked with 5% BSA for 1 h at room temperature and then incubated overnight at 4 °C with HuR antibody (1:200). The next day, cells were washed with PBS and incubated with the secondary antibody conjugated to Alexa Fluor 488 (1:600, Abcam, Cambridge, UK) for 1 h at room temperature. DAPI was used to stain the nuclear for 10 min. The fluorescence images were captured by fluorescence microscopy.

2.33. Hematoxylin and eosin (H&E) staining

Lung tissue samples were harvested from mice and immediately fixed in 10% neutral-buffered formalin for 24−48 h at room temperature. Following fixation, the tissues were dehydrated through a graded ethanol series, cleared in xylene, and embedded in paraffin. Paraffin blocks were then sectioned at a thickness of 4 μm using a microtome, and the sections were mounted on glass slides.

2.34. Flow cytometric analysis of spleen T cell population and apoptosis

Spleens were collected from sacrificed mice, and the mouse spleen cells were gently ground and passed through a 70 μm nylon cell filter to remove larger cell clumps and connective tissue. The red blood cell lysis buffer was used to lyse the residual red blood cells. After washing three times with PBS, the cells were resuspended in PBS at a concentration of 5×10^6 cells/mL. The percentage of $CD4^+$ and $CD8^+$ lymphocytes was measured by staining the cells with FITC-CD4 and APC-Cy7-CD8a (BD Pharmingen, San Diego, CA, USA). The cells were stained with Annexin V conjugated to PE to detect the apoptotic cells (Beyotime, Shanghai, China). All samples were analyzed using a BD FACScaliber flow cytometer with CellQuest Software (Beckton Dickinson, San Jose, CA, USA), and the results were analyzed with FlowJo VX10 software.

2.35. Flow cytometric assessment of spleen and blood monocyte population

The mouse spleen was digested with collagenase and DNase I for 30 min to create a single-cell suspension. The suspension was filtered through a 40 μm strainer to remove undigested fragments. Red blood cells were lysed, and the remaining splenic cells were collected by centrifugation. Whole blood samples were collected using EDTA as an anticoagulant. Immediately after centrifugation, red blood cells were lysed using a lysis buffer. After lysis, the remaining cells were washed with PBS and collected. Both splenic and blood-derived cells were stained with fluorescently labeled antibodies specific for monocyte surface markers, including CD11b, Ly6C, and Ly6G. The $CD11b^+$ $Ly6C^{hi}$ $Ly6G^{low}$ monocyte population was analyzed using flow cytometry.

2.36. Enzyme-linked immunosorbent assay (ELISA)

The TNF concentration in serum or cell culture was calculated using an ELISA kit (Neobioscience, China) and performed according to the manufacturer's instructions.

2.37. Bacterial load assay

Blood samples were collected from the orbital venous plexus of the mice. Additionally, peritoneal lavage fluid was obtained by flushing the peritoneal cavity with sterile saline. The collected blood samples were serially diluted to a concentration of 10^{-3} CFU/mL, while the peritoneal lavage fluid was diluted to 10^{-5} CFU/mL. The diluted blood and lavage fluid samples were then plated on appropriate agar media and incubated overnight at 37 °C. The number of bacterial colonies was counted the following day.

2.38. Statistical analysis

All data are presented as mean ± standard error of mean (SEM). A two-tailed Student's *t*-test was used to determine the significance of the difference between the two groups. A one-way analysis of variance (ANOVA) and Tukey's Test were used to make multiple comparisons. Survival curve comparisons were performed through

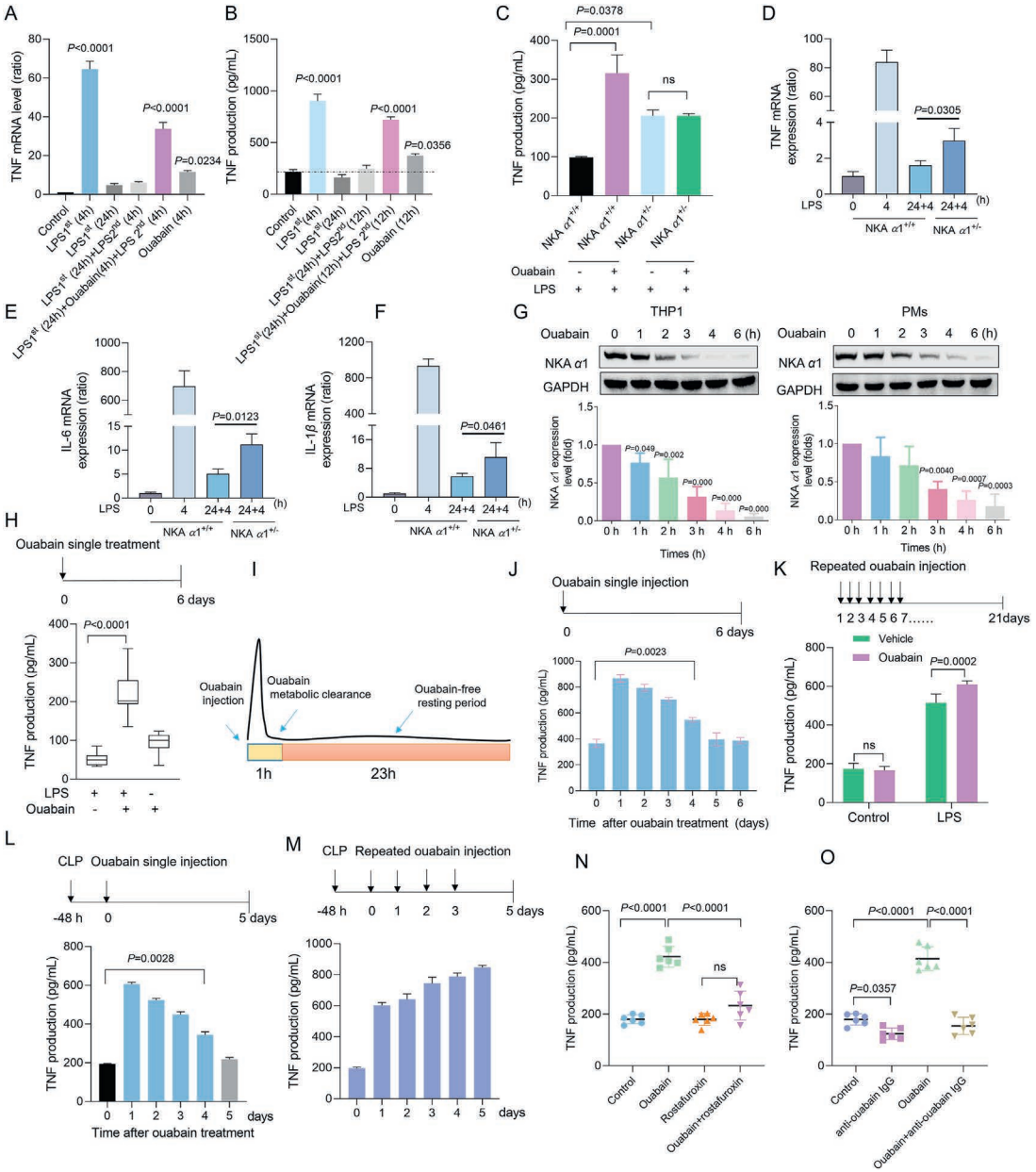

Figure 1 Ouabain induces a memory tolerance-reversing effect on IICs both *in vitro* and *in vivo*. (A) THP1 cells were subjected to a 1st LPS stimulation (1 μg/mL) for 24 h to induce tolerance, then treated with a 2nd LPS plus ouabain (50 nmol/L) for 4 or 12 h. TNF mRNA levels were measured at 4 h, and TNF production was measured at 12 h after ouabain treatment (B). Cells treated with LPS stimulation (1 μg/mL) for 4 h alone served as a positive control ($n = 3$). (C) PMs from *NKA* $\alpha1^{+/+}$ or *NKA* $\alpha1^{+/-}$ mice were treated with LPS for 24 h to induce tolerance, then received a second LPS treatment plus ouabain (50 nmol/L) for 12 h. TNF production was measured, $n = 3$. (D) PMs from *NKA* $\alpha1^{+/+}$ or *NKA* $\alpha1^{+/-}$ mice were treated with LPS for 24 h to induce tolerance, then received a second LPS treatment for 4 h. TNF, IL-6 (E), and IL-1β (F) mRNA levels were measured, $n = 3$. (G) THP-1 and PMs were treated with ouabain (50 nmol/L) for the indicated period, and then NKA α1 protein expression was examined. The quantification results are shown below ($n = 3$). (H) The tolerant human $CD14^+$ monocytes from patients with immunoparalysis (membrane HLA-DR <30%) were treated with a single dose of ouabain (50 nmol/L). Six days later, cell responsiveness to LPS was examined, as indicated by TNF production. Cells treated with ouabain but without LPS stimulation served as a control, $n = 10$. (I) Schematic illustration of the kinetic of serum ouabain after a single dose injection (i.p.) in mice. (J) Mice were injected (i.p.) with a single dose of ouabain (0.1 mg/kg). PMs from mice after ouabain injection for 0−6 days were collected and exposed to LPS stimulation (1 μg/mL) for 12 h. TNF production was measured ($n = 5$). (K) Mice were injected intraperitoneally (i.p.) with ouabain (0.1 mg/kg) daily for seven consecutive days. On the 21st day after injection, PM responsiveness to LPS was examined ($n = 5$). (L) Mice were subjected to moderate CLP and then challenged with a single dose of ouabain (0.1 mg/kg) at 48 h after CLP surgery. PMs from CLP mice, after ouabain injection for 0−5 days, were collected, and their responsiveness to LPS was examined ($n = 5$). (M) Mice were subjected to moderate CLP, then daily injected with ouabain (0.1 mg/kg) four times from 48 h after CLP surgery. PMs from CLP mice, collected after the first ouabain injection for 0−5 days, were examined for their responsiveness to LPS ($n = 5$). (N) Groups of mice were subjected to moderate CLP. Mice received saline, ouabain (0.1 mg/kg, i.p.), rostafuroxin

a Mantel-Cox log-rank test. GraphPad Prism 8 software was utilized to create graphs. The *P* value for each comparison is shown.

3. Results

3.1. Ouabain produces a lasting function-enhancing effect on peripheral IICs despite brief signaling

Ouabain was able to reverse ET on IICs[16], but whether this effect is dependent on NKA α1 remains unknown. Here, human THP-1 cells were treated with LPS for 24 h to induce tolerance, as indicated by a failure of TNF expression upon a second LPS stimulation (Fig. 1A). However, when the tolerant cells were treated with a second LPS stimulation plus ouabain, a substantial increase in TNF mRNA was observed at 4 h, accompanied by TNF protein production at 12 h (Fig. 1B). Treatment with ouabain alone also resulted in a mild increase in TNF mRNA and protein production. However, this effect contributed much less to the combined treatment. Ouabain-mediated tolerance reversal failed to occur in mouse peritoneal macrophages (PMs) isolated from *NKA* $\alpha1^{+/-}$ mice (Fig. 1C), suggesting that the effect of ouabain is critically dependent on NKA α1. Interestingly, a second LPS stimulation induced significantly higher TNF production in *NKA* $\alpha1^{+/-}$ PMs compared to that in *NKA* $\alpha1^{+/+}$ PMs, suggesting that the knockdown of *NKA* $\alpha1$ expression alone may have a tolerance-reversing effect like that of ouabain. As expected, a second LPS stimulation triggered significantly higher levels of TNF (Fig. 1D), IL-6 (Fig. 1E), and IL-1β (Fig. 1F) mRNAs in tolerant *NKA* $\alpha1^{+/-}$ PMs compared to those in *NKA* $\alpha1^{+/+}$ PMs.

Interestingly, although NKA α1 is important for ouabain's effect, a rapid and significant decline in NKA α1 protein expression occurred in both THP-1 and PMs after ouabain treatment (Fig. 1G). We therefore speculate that the effects of ouabain on reversing tolerance may not be lasting. To investigate it, the tolerant human $CD14^+$ monocytes from patients with immunoparalysis were treated with a single dose of ouabain. Then, their TNF-producing activity in response to LPS stimulation was examined by ELISA for 6 days, a duration compatible with their typical lifespan in circulation. Surprisingly, the tolerant monocytes still demonstrated increased responsiveness to LPS stimulation on the sixth day after ouabain treatment (Fig. 1H). Ouabain treatment alone, however, failed to increase TNF production significantly. Therefore, although ouabain's signaling is quickly limited by the degradation of NKA α1 within hours, it can persistently increase the responsiveness of tolerant IICs to LPS stimulation *in vitro*. Ouabain creates a memory tolerance-reversing effect on IICs.

We then tested whether the IIC's memory effect also occurs *in vivo*. Notably, ouabain metabolizes very rapidly *in vivo*, with a plasma half-life of less than 10 min after intraperitoneal (i.p.) injection[24]. Plasma ouabain is barely detectable 1 h after injection. Given this, we speculate that if ouabain is administered (i.p.) to mice for 24 h, IICs in the circulation are expected to free (unbound) ouabain exposure in plasma for less than 1 h, then recovered in ouabain-free plasma for the remaining 23 h (Fig. 1I). Following this, mice were injected (i.p.) with a single dose of 0.1 mg/kg ouabain, and the responsiveness of PMs to LPS from one to six days after injection was examined. PMs exhibited the strongest response to LPS on the first day after ouabain injection, and this effect lasted for four days (Fig. 1J). Thus, free ouabain *in vivo* can also create a memory function-enhancing effect on IICs. We presume that the gradual decline in IIC's memory effect *in vivo* may result from a complex biological environment in plasma, such as albumin binding or interference from other unknown factors, which reduces the effectiveness of free ouabain. To address this, mice were injected daily with ouabain for seven consecutive days, followed by a 14-day recovery phase. Interestingly, PMs from the mice, even after 14 days without ouabain, continued to exhibit heightened responsiveness to LPS stimulation (Fig. 1K).

We continued to investigate the *in vivo* memory effect of IIC using a murine polymicrobial sepsis model[32,34]. The CLP mice entered a state of immunoparalysis 48 h after surgery, as indicated by a decrease in inflammatory cytokine expression (TNF and IL-6) (Supporting Information Fig. S1A), an increase in bacterial burden in blood and spleen (Fig. S1B), and elevated PMs tolerance to LPS (Fig. S1C). At the 48-h mark, the CLP mice received a single dose of ouabain (0.1 mg/kg, i.p.). Consistently, PMs from ouabain-treated CLP mice over 1−5 days showed increased responsiveness to LPS (Fig. 1L). To improve the results, the CLP mice were administered ouabain four times at 24-h intervals, with the first injection beginning at 48 h post-CLP. As a result, the responsiveness of PMs to LPS was sustained and even slightly increased over time (Fig. 1M), indicating that the *in vivo* IIC's memory tolerance-reversing effect can accumulate after multiple injections. Ouabain's effect *in vivo* was significantly suppressed by its chemical blocker, rostafuroxin (Fig. 1N), and a specific neutralizing IgG (Fig. 1O), suggesting that this effect is ouabain-specific.

3.2. Ouabain has a training effect on peripheral ICs, both in vitro and in vivo

The above results suggest that ouabain may have a training-like effect on IICs. Adhering to standard protocols for immune training established in lots of other studies[41,42] (Fig. 2A), we treated the RAW264.7 cells with ouabain or β-glucan for 24 h. After treatment, the cells were recovered and rested in an ouabain-free regular medium for 1 to 5 days. On the sixth day, we treated the cells with LPS and examined their responsiveness. Like β-glucan, ouabain training significantly increased the cells' responsiveness to LPS stimulation. The surrogate markers included TNF (Fig. 2B) and IL-6 (Fig. 2C). Similar results were also observed in THP-1 cells (Fig. 2D, Supporting Information Fig. S2A) and human $CD14^+$ monocytes (Fig. S2B). Notably, as that occurred in tolerance reversal (Fig. 1C), the ouabain-mediated training effect was significantly attenuated in *NKA* $\alpha1^{+/-}$ PMs (Fig. S2C1−S2C4). Ouabain-trained cells showed elevated reactive oxygen species generation (Fig. 2E), enhanced phagocytic activity (Fig. 2F), and improved bacterial clearance (Fig. 2G) in response to LPS stimulation or bacterial infection. Interestingly, ouabain training also enhanced the responsiveness of PMs to poly (I:C) stimulation (Fig. S2D1−S2D4), suggesting that the training effect of ouabain is not stimulus-specific. Ouabain-treated cells did not exhibit a significant increase in *TNF*, *IL-6*, and *IL-1*β mRNA

(10 mg/kg, i.g.), and ouabain + rostafuroxin at 48 h after CLP. The treatments continued for 72 h, and then the PM responsiveness of each group was examined ($n = 6$). (O) Groups of mice were subjected to moderate CLP. Mice received saline, ouabain (0.1 mg/kg, i.p.), anti-ouabain IgG (100 μg per mouse, i.p.), and ouabain plus anti-ouabain IgG at 48 h after CLP. The treatments continued for 72 h; the PMs' responsiveness of each group was examined ($n = 6$).

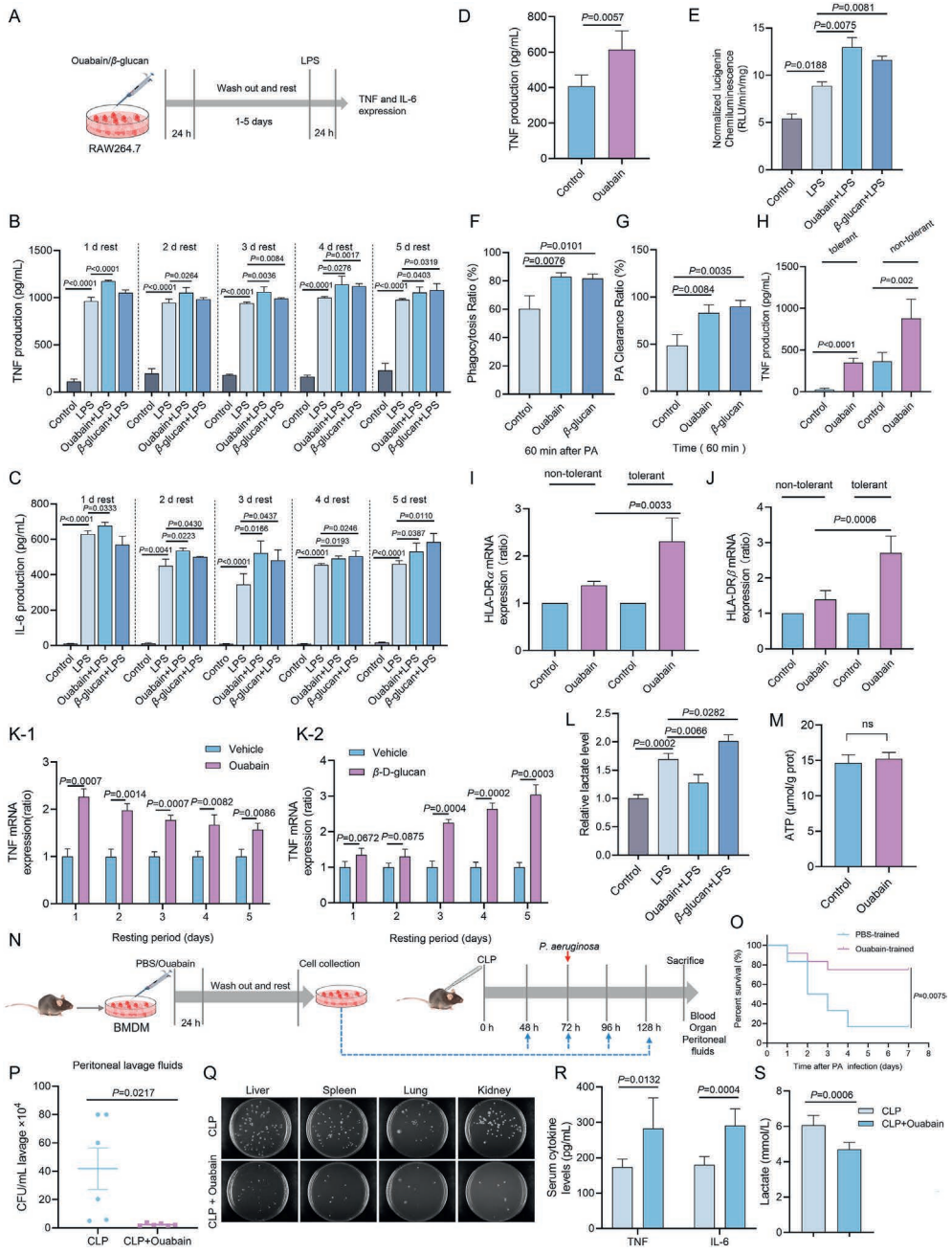

Figure 2 Ouabain has a training effect on IICs. (A) The schematic diagram of RAW264.7 cells training by ouabain or β-glucan. RAW264.7 cells were treated with ouabain or β-glucan for 24 h, then recovered in ouabain- or β-glucan-free culture medium for 1−5 days. On the sixth day, cell responsiveness to LPS, as indicated by TNF (B) and IL-6 (C) production, was examined in $n = 3$. (D) The training effect of ouabain on THP1 cells, $n = 5$. (E) PMs were treated with ouabain or β-glucan for 24 h. Following a 3-day resting period in fresh medium, cells were challenged with LPS for 12 h, harvested, and assayed for NADPH oxidase activity using lucigenin-enhanced chemiluminescence ($n = 3$). For PMs, F-G, 24 h of training with ouabain or β-glucan was followed by a 3-day resting period. The phagocytic and clearance capacity of macrophages was then assessed by infection with *P. aeruginosa* at an MOI (Multiplicity of Infection) of 10:1, $n = 3$. (F) Following 60 min of *P. aeruginosa* infection, supernatants from PMs were collected. Bacteria were plated on agar, and the phagocytosis rate was calculated based on the number of bacterial colonies. (G) Following 30 min of *P. aeruginosa* infection, PMs were treated with gentamicin (50 μg/mL) for 1 h. At 60 min post-infection, PMs were collected, lysed, and subjected to bacterial culture to examine bacterial clearance capacity. Human $CD14^+$ monocytes from healthy donors (HDs) and patients with immunoparalysis were trained with ouabain and then stimulated with LPS. The production of TNF (H), HLA-DR α (I), and HLA-DR β (J) mRNA was measured in these cells ($n = 5$). THP1 cells were trained with ouabain (K-1) or β-D-glucan (K-2) for 24 h, then allowed to recover in ouabain- or β-D-glucan-free medium for 1−5 days. TNF mRNA expression in response to LPS stimulation was then examined ($n = 3$). (L) PM cells were trained with ouabain or β-D-glucan, and cellular lactate production in the trained cells was measured after LPS stimulation, $n = 3$. (M) PM cells were trained with ouabain, and cellular ATP levels in the trained cells were measured after LPS stimulation ($n = 3$). (N) Mice after macrophage depletion were subjected to CLP surgery, followed by injection of ouabain-trained

expression before poly (I:C) stimulation, indicating that the cells returned to a normal state during the resting period. Ouabain displayed a more pronounced training effect on tolerant cells than in non-tolerant cells (Fig. 2H). Impaired HLA-DR expression on monocytes is a common feature of immunoparalysis[5,43]. Ouabain training led to increased mRNA expression of HLA-DRα/β in tolerant monocytes from patients with immunoparalysis (Fig. 2I and J), and this effect was more substantial than that in non-tolerant monocytes from healthy individuals. In summary, ouabain is a TRIM inducer. Ouabain's training effect resulted in overall functional enhancement in both tolerant and non-tolerant IICs.

Although ouabain exhibits a comparable training effect to that of β-glucan *in vitro*, we observed some differences in their training patterns (Fig. 2B and C). Ouabain-trained cells respond quickly to LPS stimulation after just one day of rest. In contrast, β-glucan-trained cells require 2 to 3 days of rest to enhance their responsiveness. To further explore this difference, we utilized TNF mRNA levels as an earlier marker than TNF protein production to compare their effects. Again, ouabain-trained cells responded more rapidly to LPS stimulation than β-glucan-trained cells (Fig. 2K−1 and K-2). In addition, β-glucan training enhanced lactate production. In contrast, ouabain training reduced lactate production (Fig. 2L) and did not significantly affect cellular ATP content (Fig. 2M). Thus, ouabain differs from β-glucan in training behaviors regarding response speed and energy metabolism.

To investigate whether the training effect of ouabain is beneficial for bacterial clearance *in vivo*, mice were treated with clodronate liposomes to deplete macrophages. Subsequently, these mice were subjected to CLP surgery and adoptively transferred with ouabain-trained bone marrow-derived macrophages (BMDMs) (Fig. 2N)[36]. *P. aeruginosa* (PA) was introduced 72 h after CLP to enhance the severity of infection. Notably, the adoptive transfer of ouabain-trained BMDMs significantly decreased the mortality rate of CLP mice, achieving a survival rate around 80% (Fig. 2O), resulted in a notable reduction in bacterial loads in peritoneal lavage fluids (Fig. 2P) and in organs including the liver, lungs, spleen, and kidneys (Fig. 2Q, Fig. S2E1−S2E4), increased the production of serum TNF and IL-6 (Fig. 2R), while simultaneously decreasing serum lactate levels (Fig. 2S).

3.3. PKCα/HuR-involved posttranscriptional regulatory mechanism regulates ouabain's training effect

Ouabain is a hormone-like small molecule with low immunogenicity. Hormones tend to have potent but short-lived effects, allowing for precise regulation with minimal side effects[44]. The rapid and intense training effects of ouabain suggest that it might activate specific stressful mechanisms to have function. A previous study suggests that a stress-related RNA-binding protein, human antigen R (HuR), plays a critical role in cytokine production mediated by ouabain[16]. However, whether HuR is involved in TRIM remains completely unknown. Here, in line with previous investigations[16], we observed a significant time-dependent export of HuR from the nucleus in ouabain-treated tolerant cells, as indicated by the cytoplasmic-to-nuclear HuR ratio (Fig. 3A). Ouabain training also led to a significant cytoplasmic HuR distribution (Fig. 3B). Additionally, the cytoplasmic-to-nuclear HuR ratio in *NKA* $\alpha 1^{+/+}$ PMs was significantly lower than that in *NKA* $\alpha 1^{+/-}$ PMs, suggesting that NKA α1 knockdown also contributes to the translocation of HuR to the cytoplasm (Fig. 3C). Ouabain's training effect was significantly diminished in HuR-deficient macrophages (Fig. 3D). As a result, the beneficial effect of ouabain-trained macrophages on CLP mice was largely attenuated when HuR expression was deleted (Fig. 3E).

Given the role of HuR in ouabain's training effect, we aimed to understand the underlying mechanism. Protein kinases are known to regulate the nucleocytoplasmic shuttling of HuR. We found that Gö6983, a PKC inhibitor, significantly inhibited the nuclear export of HuR mediated by ouabain (Fig. 3F). Further analysis indicated that PKCα played a crucial role in this process (Fig. 3G). HuR can bind to the AU-rich elements (AREs) in the 3′-UTR of target mRNAs to modulate their stability and/or translation efficacy[45,46]. In our study, the increase in luciferase fluorescence from the 3′-UTR of *TNF* mRNA induced by ouabain was almost completely suppressed in cells where PKCα was silenced (Fig. 3H). We also observed a decrease in the phosphorylated form of PKCα in the cytoplasm. At the same time, its levels increased in the nuclei of ouabain-treated cells (Fig. 3I). Further analysis revealed that ouabain enhanced the interaction between HuR and PKCα within the nucleus (Fig. 3J). Additionally, intracellular Ca^{2+} levels regulate the activation of PKCα and the nuclear export of HuR induced by ouabain (Fig. 3K and L). PKCα interacts with HuR at serine residues 158 and 221[47]. Here, serine 221 in HuR is critical for the ouabain-induced nuclear export of HuR and the increased luciferase activity of TNF 3′-UTR (Fig. 3M and N). PKCα activity was impaired in cells with ET *in vitro* [48]. However, ouabain treatment reactivated PKCα phosphorylation in tolerant cells (Fig. 3O and P).

3.4. lncRNA-CYTOR plays a crucial role in ouabain's training effect by sequestering HuR in the cytoplasm

Notably, HuR is a protein that rapidly shuttles between the nucleus and cytoplasm, quickly returning to the nucleus upon stimulus withdrawal. Ouabain leads to a rapid degradation of NKA α1 (Fig. 1G) and a temporary upregulation of PKCα (Fig. 3I), suggesting that HuR is unlikely to stay in the cytoplasm for long. Unexpectedly, we observed that the levels of cytoplasmic HuR were persistently increased in ouabain-treated tolerant cells, even after ouabain was withdrawn for 12 h (Fig. 4A). In training experiments, HuR remained in the cytoplasm even five days after ouabain withdrawal (Fig. 3B). This implies that HuR may be hijacked in the cytoplasm of ouabain-trained cells. To confirm it, we treated cells with PMA, a PKCα activator, which resulted in HuR nuclear export levels comparable to those seen with ouabain treatment. In PMA-treated cells, cytoplasmic HuR rapidly shuttled back to the nucleus after PMA withdrawal. In contrast, a significant fraction of HuR proteins were retained in the cytoplasm of ouabain-treated cells even after withdrawal (Fig. 4B). We hypothesized that the cytoplasmic retention of HuR could be related to its RNA-binding properties. To test this hypothesis, we

BMDMs at 48, 72, 96, and 120 h post-CLP. *P. aeruginosa* infection was conducted at 72 h post-CLP. The animals' survival rate (O), bacterial counts in peritoneal lavage fluids (P), and organs, including livers, lungs, spleens, and kidneys, were examined (Q). Serum expression levels of TNF, IL-6 (R), and lactate (S) were also examined ($n = 6$).

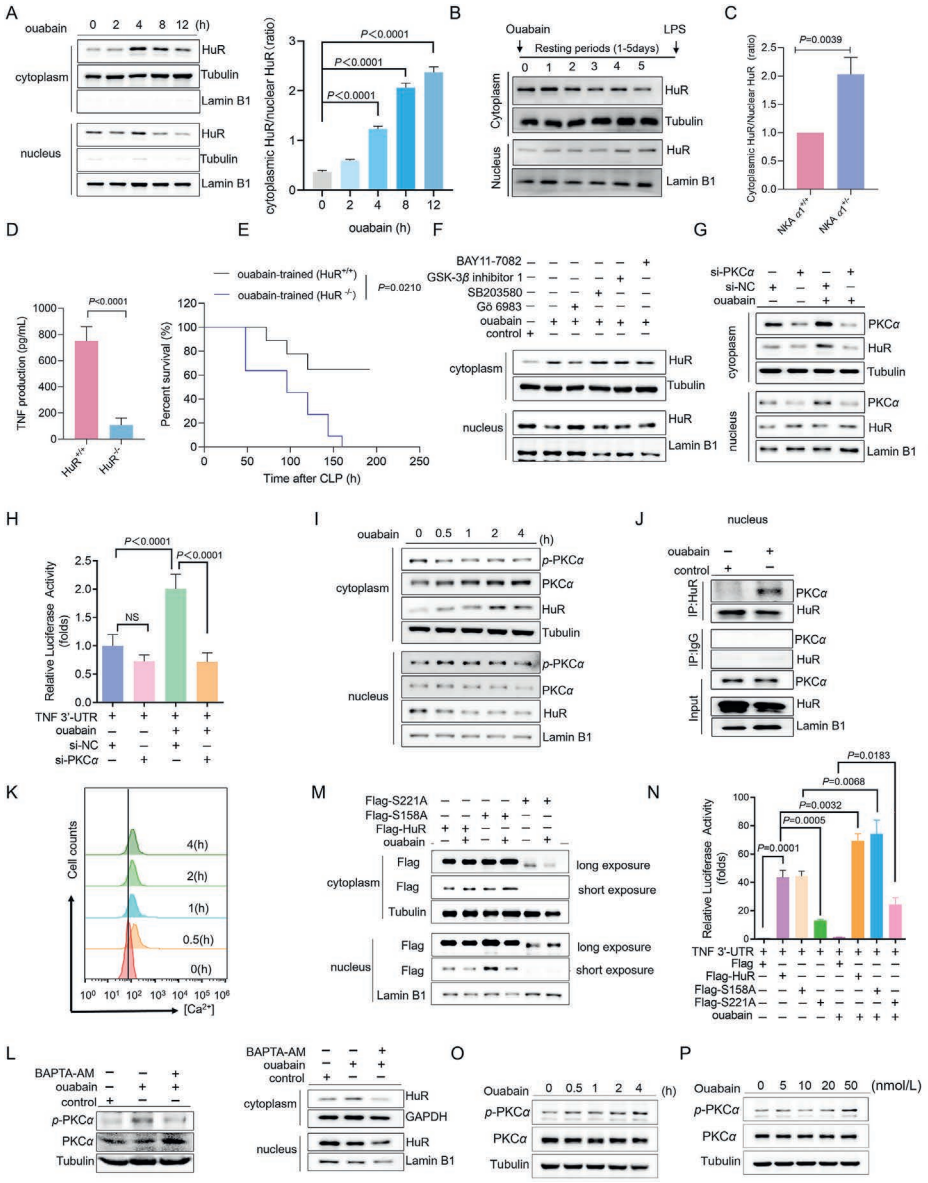

Figure 3 PKCα-dependent HuR nuclear export is involved in the ouabain's training effect. (A) The tolerant THP1 cells were treated with 50 nmol/L ouabain at different times. The expression of cytoplasmic or nuclear HuR was examined by Western blot analysis, and the quantification results are shown on the right, $n = 3$. (B) THP1 cells were trained with 50 nmol/L ouabain for 24 h, then recovered for 1−5 days. The expression of cytoplasmic and nuclear HuR was examined. (C) The cytoplasmic and nuclear HuR expressions were examined in PMs from *NKA* $\alpha 1^{+/+}$ and *NKA* $\alpha 1^{+/-}$ mice ($n = 3$). (D) PMs from HuR^{WT} and $HuR^{-/-}$ RAW264.7 cells were trained with ouabain, $n = 6$. (E) Groups of mice were treated with liposomes to deplete macrophages, followed by a moderate CLP and *S.tm.* (2×10^3 CFU, i.p.) infection (72 h post-CLP). At 48 h post-CLP, mice were adoptively transferred with ouabain-trained HuR^{WT} or $HuR^{-/-}$ RAW264.7 cells, and the treatments were repeated three times at 72, 96, and 120 h post-CLP, with $n = 10$ mice per group. (F) THP1 cells were pre-treated with the SB203580 (p38 MAPK inhibitor), Gö6983 (protein kinase C inhibitor), BAY11-7082 (IkB kinase α inhibitor), and GSK-3β inhibitor 1 for 2 h. The expression of cytoplasmic or nuclear HuR was examined. (G) THP1 cells were transfected with si-NC or si-PKCα for 36 h and then incubated with or without 50 nmol/L ouabain for 12 h. The expression of cytoplasmic and nuclear PKCα or HuR was examined. (H) The HEK293T cells, after transfection with a TNF 3′-UTR luciferase reporter and siRNAs against PKCα, were treated with 50 nmol/L ouabain for 12 h, and the luciferase activity of the si-NC group was set at 1.0 ($n = 3$). (I) THP1 cells were treated with ouabain at 50 nmol/L for different periods, and the protein expression of p-PKCα, PKCα, and HuR in cytoplasmic and nuclear fractions were examined. (J) THP1 cells were treated with 50 nmol/L ouabain for 12 h, and the protein lysates of nuclear fractions were immunoprecipitated with control IgG or anti-HuR IgG overnight. The protein expressions of PKCα and HuR in the immunoprecipitate were examined. (K) THP1 cells were treated with 50 nmol/L ouabain for the indicated periods. Cells were incubated with Fluo-4 AM for 60 min at 37 °C, and the fluorescence intensity in the FL1 channel was detected using a flow cytometer. (L) THP1 cells were pre-treated with the calcium chelator BAPTA-AM (10 μmol/L) for 2 h before the addition of ouabain (50 nmol/L). (M) The HEK293T cells were transfected with Flag-tagged HuR and its mutants for 24 h, then treated with or without 50 nmol/L ouabain for 12 h. HuR expressions in the cytoplasmic and nucleus fractions were examined. (N) The HEK293T cells were transfected with the indicated constructs, and luciferase

performed microarray analysis to identify differentially expressed RNAs in ouabain-treated peripheral blood mononuclear cells (PBMCs) from patients with immunoparalysis. The results indicated that the expression of four long noncoding RNAs (lncRNAs), including MALAT1, UCA1, DLEU2, and CYTOR, were significantly upregulated by ouabain, with CYTOR showing the highest expression level (Fig. 4C). RNA sequencing analysis revealed that CYTOR was preferentially expressed in the bone marrow, lymph nodes, and spleen, suggesting its potential role in regulating immunity (Supporting Information Fig. S3A). lncRNAs can significantly influence the cellular distribution of proteins[49]. We found HuR expression was not significantly affected by CYTOR silencing (Fig. S3B and S3C); however, CYTOR silencing significantly suppressed the cytoplasmic retention of HuR in ouabain-treated cells (Fig. 4D and E). Furthermore, in CYTOR-silenced cells, HuR rapidly translocated back to the nucleus after ouabain withdrawal (Fig. 4F−1 and F-2).

CYTOR has five variants, and we only confirmed the presence of CYTOR variant three in THP-1 cells (Fig. S3D). CYTOR contains a short open reading frame (ORF) of 249 nucleotides; however, we established that this ORF could not lead to polypeptide translation (Fig. S3E1−S3E3). CYTOR was predominantly distributed in the cytoplasm of both immune and non-immune cells (Fig. 4G, Fig. S3F). In ouabain-treated tolerant cells (Fig. 4H, Fig. S3G), CYTOR co-localized with cytoplasmic HuR; further analysis revealed that both TNF mRNA and CYTOR were immunoprecipitated using an anti-HuR IgG in ouabain-treated cells (Fig. 4I). The binding of CYTOR to HuR significantly diminished when the RNA recognition motif 3 (RRM3) domain of HuR was deleted (Fig. 4J, Supporting Information Fig. S4A). Moreover, the RRM3 domain of HuR alone is sufficient for binding to CYTOR (Fig. 4K, Fig. S4B). Using RNAfold software, we predicted a secondary structure for CYTOR, with the lowest free energy calculated at −160.10 kcal/mol (Fig. 4L). HuR interacts with the sense strand of CYTOR (Fig. 4M) and binds to a CYTOR deletion mutant that contains nucleotides 1-48 (Fig. 4N and O, Fig. S4C−S4F). This segment contains two stem-loops (Fig. 4L). When we introduced mutations into the loop region, the interaction between HuR and CYTOR was significantly reduced (Fig. 4P, Fig. S4G). The HuR-binding stem-loop structure of CYTOR is highly conserved across species, particularly among primates (Fig. 4Q).

3.5. *CYTOR links immune tolerance and trained immunity*

Ouabain-mediated reversal of tolerance was almost entirely abolished in cells after CYTOR silencing (Fig. 5A). In the training experiment, the effect of ouabain on CYTOR expression (Fig. 5B) positively correlated with its training effect (Fig. 2K−l) and cytoplasmic HuR abundance (Fig. 3B). Notably, CYTOR was also upregulated in β-D-glucan-trained cells (Supporting Information Fig. S5A). However, this increase lagged behind that observed with ouabain, and further, β-D-glucan-training failed to induce significant HuR nuclear export (Fig. S5B and S5C). The training effect of ouabain was significantly diminished in CYTOR-silenced cells (Fig. 5C). Furthermore, overexpression of CYTOR alone resulted in increased *TNF*, *IL-6*, and *IL-1β* mRNAs (Fig. S5D1−S5D3) and enhanced responsiveness to LPS (Fig. 5D). This indicates that CYTOR plays a crucial role in the training effect of ouabain. Interestingly, the expression of CYTOR initially increased and then gradually decreased in LPS-treated monocytes (Fig. 5E), mirroring the expression pattern of TNF (Fig. S8C-1). CYTOR expression increased in monocytes from patients with sepsis but decreased in patients with immunoparalysis, which coincided with a reduction in TNF expression (Fig. 5F). Single-cell sequencing analysis, as detailed in the GSE167363 datasheet, also confirmed these findings (Fig. 5G). Therefore, CYTOR is a crucial long noncoding RNA that connects TRIM and immune tolerance.

Both ouabain and β-D-glucan trigger the production of CYTOR in training experiments *in vitro*, we, therefore, investigated and compared their effects on bacterial clearance *in vivo*. Notably, the results showed that ouabain (0.1 mg/kg) was more effective than β-D-glucan (10 mg/kg) in improving animal survival (Fig. 5H) and bacterial clearance (Fig. 5I) when administered at a concentration of one percent of β-D-glucan. Further, ouabain enhanced the effect of β-D-glucan and their combined administration led to a survival rate of approximately 90% in CLP models (Fig. 5H). Ouabain also enhanced the effect of β-D-glucan on the clearance of bacteria from both the peritoneal fluid and the blood (Fig. 5I). Similar outcomes were also observed in terms of lung injury reduction, as evidenced by the presence of cleaved caspase 3 (Fig. 5J), the severity of inflammatory cell infiltration in lung tissue (Fig. 5K), and TNF mRNA expression in the lung and liver (Fig. 5L).

3.6. *CYTOR helps stabilize pro-inflammatory and immunostimulatory cytokine mRNAs in ouabain-trained IICs*

The 3′-UTRs of cytokines, including TNF, IL-6, IL-1β, GM-CSF, and IFN-γ, all contain typical AU-rich elements (AREs) that are capable of binding to HuR[45]. Among those cytokines, TNF, IL-6, and IL-1β are frequently used surrogate markers for TRIM, as shown in this study. On the other hand, TNF, GM-CSF, and IFN-γ have demonstrated significant immunoparalysis-reversing effects in either preclinical studies or small-scale clinical trials[43]. We, therefore, speculate that CYTOR may help stabilize the mRNAs of these immunostimulatory cytokines. The results demonstrated that the half-lives of TNF (Fig. 6A), GM-CSF (Fig. 6B), and IFN-γ (Fig. 6C) mRNAs in ouabain-trained monocytes after LPS stimulation were significantly prolonged, an effect that was notably diminished after CYTOR expression silencing. It is important to note that the mRNA stability of those genes in ouabain-trained cells, when not stimulated by LPS, did not show a significant increase compared to control cells. This suggests that LPS stimulation can quickly mobilize CYTOR in the cytoplasm to stabilize the mRNAs.

Among those cytokines, TNF plays critical roles in immune recovery[50] and immunoparalysis reversal[16,51]. Therefore, we selected TNF as a representative and examined how CYTOR affects the stability of TNF mRNA. CYTOR forms a ternary complex with HuR and TNF mRNA (Fig. 4I), suggesting that CYTOR and HuR may work together to enhance TNF mRNA stability. Overexpression of CYTOR increased the levels of TNF 3′-UTR reporter constructs. However, this effect was significantly reduced

activity was measured using a dual-luciferase reporter assay ($n = 3$). (O) The tolerant THP1 cells were treated with 50 nmol/L ouabain for different periods, and the protein expressions of p-PKCα and PKCα were examined. (P) The tolerant THP1 cells were treated with ouabain at the indicated concentrations for 4 h, $n = 3$.

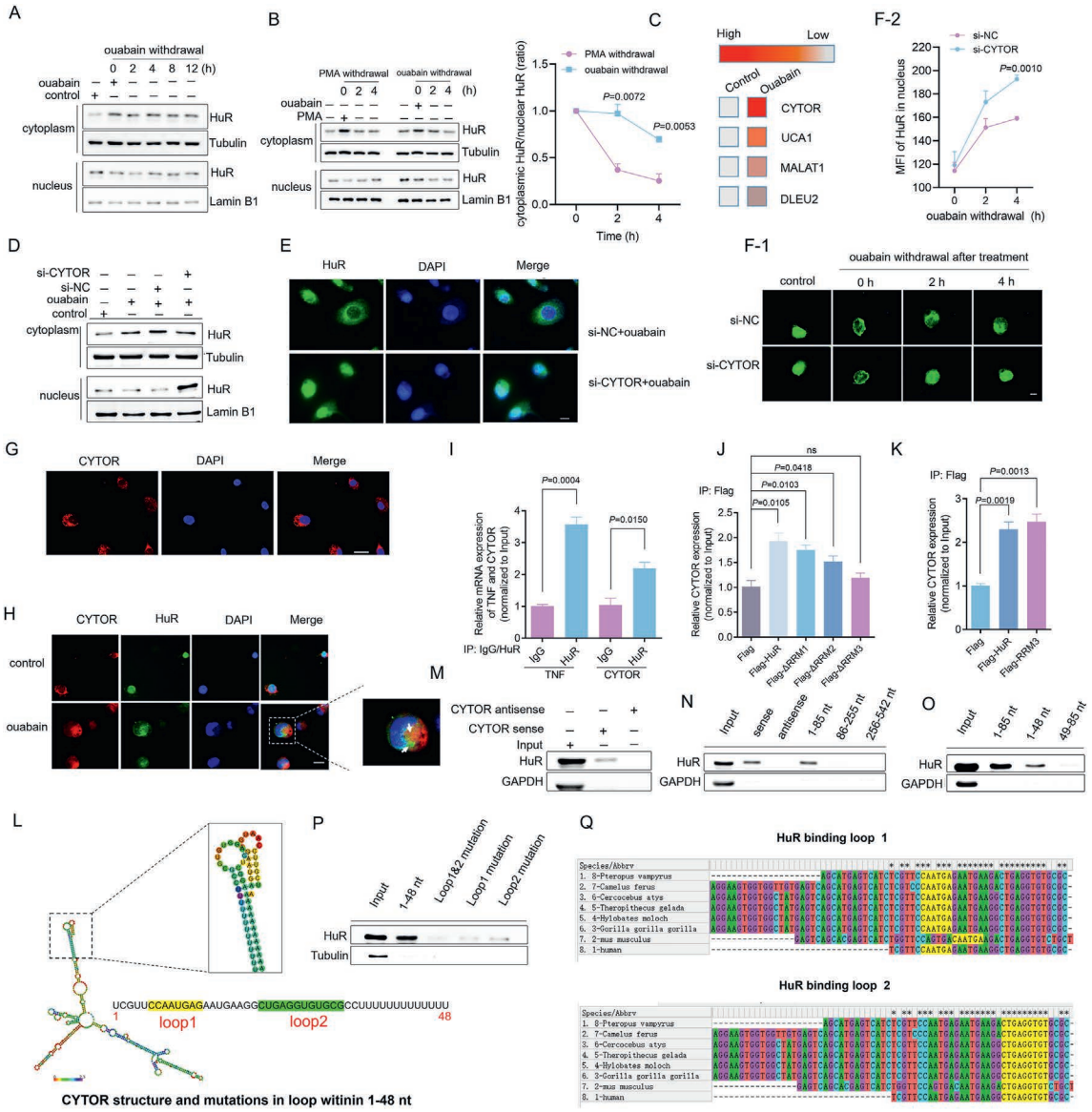

Figure 4 CYTOR interacts with and hijacks HuR in the cytoplasm of ouabain-treated cells. (A) LPS-tolerized THP1 cells were treated with 50 nmol/L ouabain for 12 h, and ouabain was then withdrawn for the indicated periods (2−12 h). (B) THP1 cells were treated with 100 ng/mL PMA for 4 h or 50 nmol/L ouabain for 12 h, and PMA or ouabain was then withdrawn for 2 and 4 h (left). The kinetics of HuR nucleo-cytoplasm shuttling are presented on the right, $n = 3$. (C) PBMCs from patients with immunoparalysis were treated with ouabain for 8 h, and microarray analysis was performed to examine the differentially expressed RNAs. LncRNAs that were upregulated by ouabain were listed. LPS-tolerized THP-1 cells were transfected with siRNAs against CYTOR and subsequently treated with 50 nmol/L ouabain for 12 h. HuR protein expression in the cytoplasm and nucleus was examined (D), and the cellular distribution of HuR was examined by immunofluorescence assay (E) (scale bar = 20 μm). (F-1) THP1 cells were transfected with siRNAs against CYTOR for 36 h, then received LPS to induce tolerance. The tolerant THP-1 cells were treated with ouabain for 12 h, then ouabain was withdrawn from the culture medium for 2 and 4 h. The cellular distribution of HuR was examined using an immunofluorescence assay (scale bar = 20 μm). (F-2) The kinetics of HuR shuttling back to the nucleus after ouabain withdrawal. (G) The cellular distribution of CYTOR in THP1 cells was examined using an RNA-FISH assay. CYTOR expression is indicated in red (scale bar = 20 μm), $n = 3$. (H) THP1 cells were treated with or without 50 nmol/L ouabain for 12 h, and RNA-FISH and immunofluorescence assay were utilized to examine the co-localization of HuR and CYTOR, HuR expression is indicated in green, and CYTOR expression is indicated in red (scale bar = 20 μm). (I) The whole cell lysates of ouabain-treated THP1 cells were immunoprecipitated using control IgG or anti-HuR IgG, and the presence of TNF mRNA and CYTOR in the immunoprecipitate was measured, $n = 3$. (J) HuR deletion mutants were transfected into HEK293T cells for 48 h, and a RIP assay was used to detect CYTOR binding to HuR deletion mutants, $n = 3$. (K) The HEK293T cells were transfected with HuR or RRM3 of HuR, and a RIP assay was used to detect CYTOR binding to HuR-RRM3, $n = 3$. (L) The predicted secondary structure of CYTOR and the loop structure in nucleotides from 1 to 48. (M) The interaction between HuR and the sense or antisense strand of CYTOR as detected by RNA pull-down assay. (N) The interaction between HuR and CYTOR deletion mutants includes 1−85 nt, 86−255 nt, and 256−542 nt. (O) The interaction between HuR and CYTOR deletion mutants includes 1−85 nt, 1−48 nt, and 49−85 nt. (P) The interaction between HuR and CYTOR variants with mutations in loop structure (1−48 nt). (Q) Highly conserved HuR-binding stem-loop structure in CYTOR across species, the conserved loop1 sequence "CAATGA" and loop2 sequence "CTGAGGTG" are indicated in yellow.

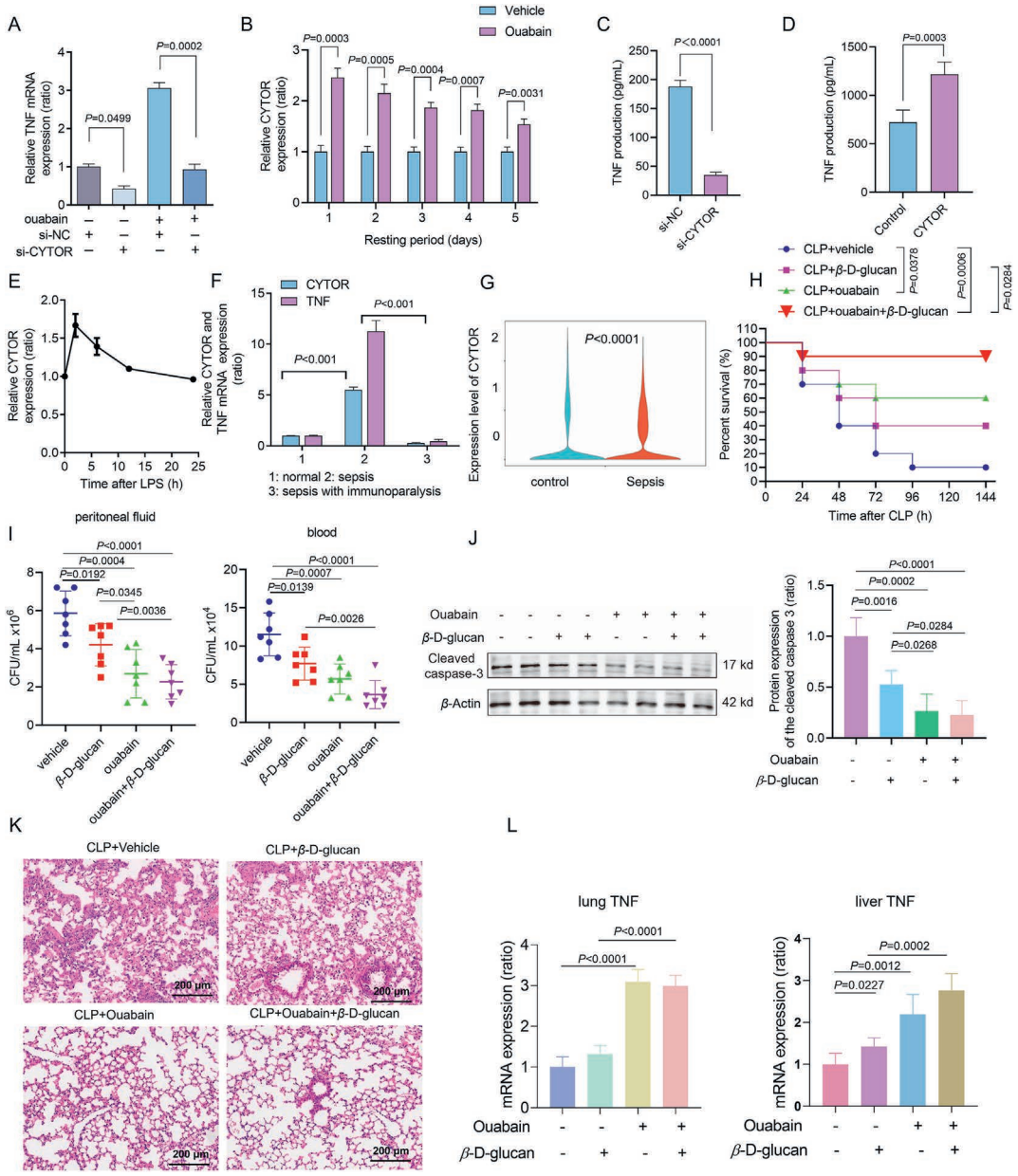

Figure 5 CYTOR links immune tolerance and trained immunity. (A) LPS-tolerized THP1 cells were transfected with si-NC or si-CYTOR and then further treated with 50 nmol/L ouabain for 4 h, $n = 3$. (B) THP1 cells were trained with ouabain at 50 nmol/L for 24 h, then allowed to recover in the ouabain-free medium for 1−5 days. CYTOR production was examined ($n = 5$). (C) CYTOR-silenced THP-1 cells were subjected to LPS-induced tolerance, followed by ouabain (50 nmol/L) treatment, $n = 3$. (D) RAW264.7 cells were transfected with CYTOR for 24 h, and both the control and CYTOR-transfected cells were subjected to LPS treatment for an additional 12 h. TNF production was then examined ($n = 3$). (E) THP1 cells were treated with LPS for the indicated time. (F) The expression levels of CYTOR and TNF mRNA in PBMCs from healthy donors and patients with sepsis or sepsis-induced immunoparalysis, $n = 3$. (G) CYTOR expression in monocytes from healthy donors and patients with sepsis, as determined by single-cell RNA sequencing analysis. (H) CLP mice received ouabain (0.1 mg/kg) or β-D-glucan (10 mg/kg) individually or in combination at 6, 12, and 18 h after CLP surgery, $n = 10$. (I) The bacterial loads in peritoneal lavage fluid and blood of CLP mice, $n = 7$−8. (J) The expression levels of the cleaved caspase-3 in the lung tissue from CLP mice, $n = 3$. (K) Representative H&E-stained lung tissue sections, indicating the effects of ouabain, β-D-glucan, and their combination on CLP-induced lung injury, scale bar = 200 μm, $n = 5$. (L) Effects of ouabain and β-D-glucan on TNF mRNA expression in lung and liver tissues from CLP models, $n = 5$.

when the HuR-binding loop structure of CYTOR was mutated (Fig. 6D). The core structure of the TNF 3′-UTR contains multiple copies of AREs that HuR can bind. However, the continuity of these AREs is disrupted by a potential binding site for miR-181d-5p (UGAAUGU), indicating a competition between HuR and miR-181d-5p for binding to the TNF 3′-UTR (Fig. 6E). It is important to note that miR-181d is critically involved in immunoparalysis and LPS-induced tolerance by promoting TNF mRNA degradation[16]. Interestingly, CYTOR contains a sequence of nucleotides (5′-ACAUUC-3′) that is identical to the seed sequence of

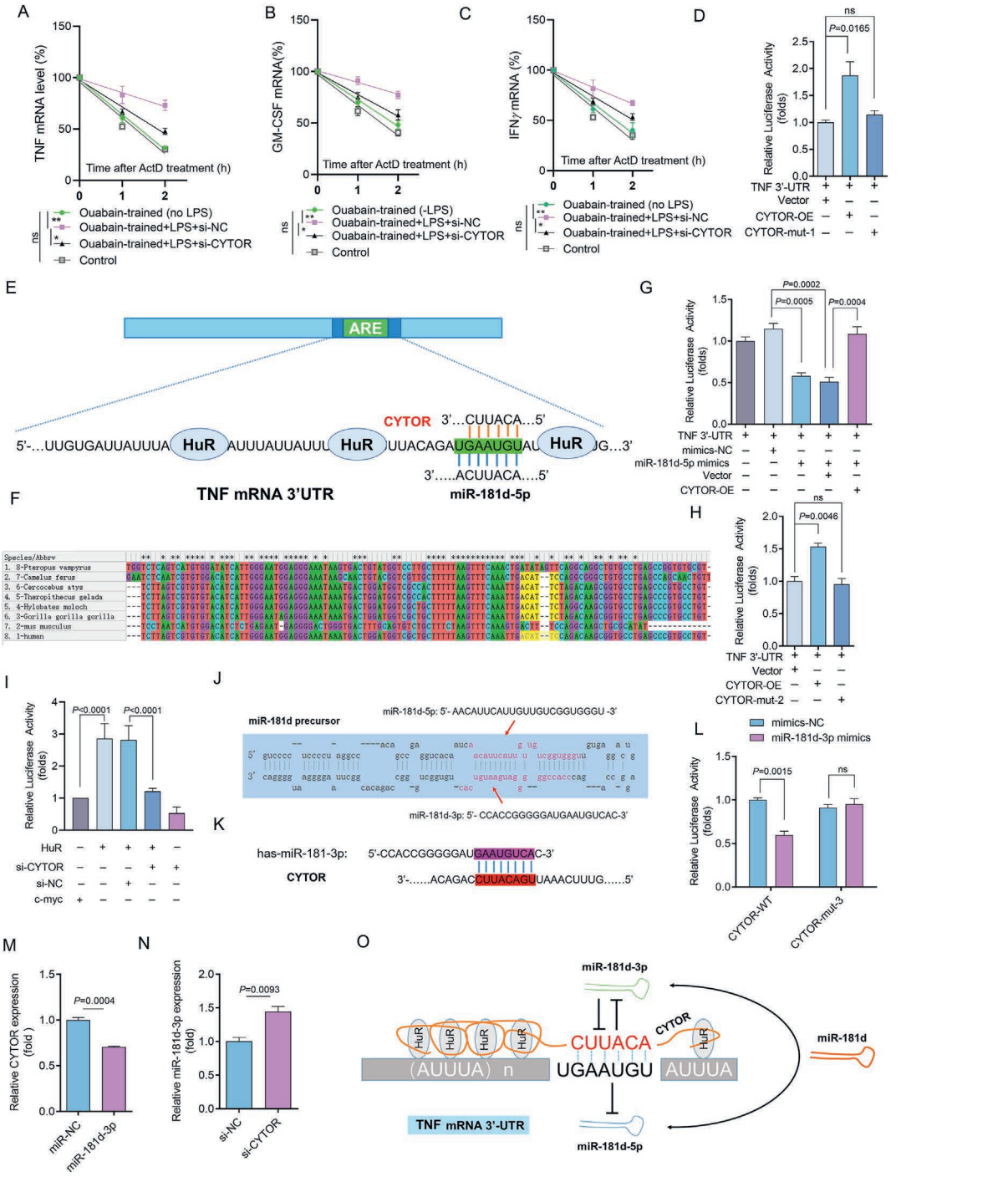

Figure 6 CYTOR synergizes with HuR but competes with miR181d-5/3p over TNF 3′-UTR. (A) THP1 cells were transfected with siRNAs against CYTOR and trained with ouabain (50 nmol/L) for 3 days. After training, cells were stimulated with LPS for 4 h, then challenged with ActD (5 μg/mL) for 1−2 h to terminate gene transcription and observe mRNA decay, TNF (A), GM-CSF (B), and IFN-γ (C) mRNAs were examined, $n = 3$, $^*P < 0.05$, $^{**}P < 0.01$, ns = no significant. (D) The HEK293T cells were transfected with a TNF 3′-UTR reporter and CYTOR or CYTOR variant with a mutation in the HuR binding loop structure (CYTOR-mut-1), $n = 3$. (E) The TNF 3′-UTR contains multiple copies of AREs and potential CYTOR or miR-181d-5p binding sites. (F) Conserved TNF 3′-UTR binding site on CYTOR across species. (G) HEK293T cells were transfected with CYTOR, miR-181d-5p mimics, and a TNF 3′-UTR reporter, $n = 3$. (H) HEK293T cells were transfected with a TNF 3′-UTR reporter and CYTOR or CYTOR variant with a mutation in the TNF 3′-UTR binding site (CYTOR-mut-2). (I) HEK293T cells were transfected with TNF 3′-UTR reporter, HuR-expressing plasmid, and siRNAs against CYTOR. (J) miR181-d and its progeny miRNAs. (K) miR-181d-3p base pairs with CYTOR. (L) HEK293T cells were transfected with the CYTOR or CYTOR variant with mutation in miR-181d-3p binding site (CYTOR-mut-3) along with miR-181d-3p mimics. CYTOR and its mutant were cloned into the pGL3-Basic vector downstream of the firefly luciferase gene ($n = 3$). (M) The THP1 cells were transfected with miR-181-3p mimics. (N) The THP1 cells were transfected with siRNAs against CYTOR. (O) Schematic depiction of cooperation between CYTOR and HuR and competition between CYTOR and miR-181d-5p/3p over TNF 3′-UTR.

miR-181d-5p for TNF 3′-UTR binding. This nucleotide sequence is highly conserved across species, particularly in primates (Fig. 6F). Additionally, the inhibitory effect of miR-181d-5p on TNF 3′-UTR reporter activity was significantly reversed by CYTOR (Fig. 6G). The stimulatory effect of CYTOR on TNF 3′-UTR reporter activity was almost entirely suppressed when the "ACAUUC" sequence was mutated (Fig. 6H). Thus, CYTOR antagonizes the binding of miR-181d-5p to the TNF 3′-UTR. Further, the effect of HuR overexpression on TNF 3′-UTR reporter activity was significantly attenuated following CYTOR silencing (Fig. 6I), suggesting CYTOR acts as an RNA rope to tightly bind HuR to the AREs of the TNF 3′-UTR.

The precursor miR-181d can be processed into two forms: miR-181d-3p and miR-181d-5p; miR-181d-5p is base-paired with miR-181d-3p (Fig. 6J). Interestingly, eight nucleotides in miR-181d-3p perfectly base-pairs with CYTOR (Fig. 6K). The introduction of miR-181d-3p mimics inhibited the effect of CYTOR on the TNF 3′-UTR reporter activity. However, this inhibition was eliminated when the miR-181d-3p binding site on CYTOR was mutated (Fig. 6L). Furthermore, overexpressing miR-181d-3p resulted in a decreased expression of CYTOR (Fig. 6M), while silencing CYTOR led to an increase in miR-181d-3p expression (Fig. 6N). In summary, while the binding of miR-181d-5p to the TNF 3′-UTR was antagonized by CYTOR, its counterpart, miR-181d-3p, subsequently suppressed the effect of CYTOR. Therefore, CYTOR interacts with HuR but competes with both miR-181d-5p and miR-181d-3p to enhance the stability of TNF mRNA (Fig. 6O).

3.7. Ouabain increases CYTOR production via an EGFR/AP-1/CYTOR/EGFR self-amplifying circuit

The above results suggest that to sustain the training effect, CYTOR production needs to be enhanced by ouabain to counteract the effects of miR-181d-5p/3p. Ouabain increases CYTOR production at the transcriptional level (Fig. 7A) but not at the posttranscriptional level (Supporting Information Fig. S6A). To investigate the underlying mechanism, we constructed various deletion mutants of the CYTOR promoter (Fig. 7B). The promoter region from −107 to −53 is critical for ouabain-induced CYTOR transcription (Fig. 7C). This region contains two putative activator protein-1 (AP-1) binding sites (Fig. S6B). The luciferase activity of the CYTOR promoter was significantly reduced when these two putative AP-1 binding sites were mutated (Fig. 7D). Additionally, ouabain increased the luciferase activity of the AP-1 reporter in a time-dependent manner (Fig. S6C). In cells with reduced expression of c-Fos or c-Jun, the ouabain-induced production of CYTOR was significantly diminished (Fig. 7E and F). Chromatin immunoprecipitation (ChIP) analysis further confirmed that ouabain treatment promoted the binding of c-Fos and c-Jun to the CYTOR promoter (Fig. 7G). Upon binding to NKA α1, ouabain initiates signaling events that lead to EGFR phosphorylation[52]. The increase in both AP-1 luciferase activity (Fig. S6D) and CYTOR transcription (Fig. 7H) induced by ouabain was significantly inhibited by erlotinib, an EGFR tyrosine kinase inhibitor. Moreover, CYTOR induction by ouabain was also significantly reduced in cells with decreased expression of the NKA α1 (Fig. 7I). In summary, the transcription of CYTOR induced by ouabain is primarily mediated by the NKA α1/EGFR/AP-1 signaling cascade.

Interestingly, although EGFR is required for CYTOR expression, CYTOR also regulates EGFR protein expression (Fig. 7J, Fig. S6E). The ouabain-induced increase in EGFR expression was significantly reduced after CYTOR silencing (Fig. 7K). CYTOR silencing in cells shortened the half-life of the EGFR protein (Fig. 7L). Furthermore, CYTOR silencing enhanced EGFR ubiquitination in the presence of proteasomal inhibitor MG132 (Fig. 7M). CYTOR silencing-induced EGFR degradation was significantly prevented by MG132 but not by lysosomal inhibitor E64D (Fig. 7N). Therefore, CYTOR stabilizes EGFR protein by preventing ubiquitin-mediated degradation. EGFR phosphorylation at tyrosine Y1045 induces self-degradation through direct binding to the ubiquitin E3 ligase C-Cbl[53]. In contrast, EGFR phosphorylated at Y1068 binds indirectly to C-Cbl *via* Grb2 to promote self-degradation (Fig. S6F)[53]. Our findings indicate that ouabain treatment resulted in significant phosphorylation of EGFR at Y1068, while it time-dependently suppressed phosphorylation at Y1045 (Fig. 7O). This result suggests that the production of CYTOR induced by ouabain is mediated by EGFR that is phosphorylated at Y1068 rather than at Y1045. Notably, levels of EGFR phosphorylated at Y1045 began to decrease 1 h after treatment in ouabain-treated cells. However, total EGFR protein levels did not increase until 8−12 h, when the levels of EGFR phosphorylated at Y1068 gradually decreased. This finding suggests that EGFR phosphorylated at Y1068 plays a crucial role in regulating EGFR turnover in ouabain-treated cells. Additionally, we observed increases in both EGFR/C-Cbl (Fig. 7P) and EGFR/Grb2 interactions (Fig. 7Q) following silencing of CYTOR. This finding suggests that CYTOR may bind to the shared EGFR protein. RIP experiments confirmed that the sense strand of CYTOR was bound to EGFR (Fig. 7R).

Overall, ouabain induces the phosphorylation of EGFR at Y1068, leading to increased transcription of CYTOR. In turn, CYTOR binds to EGFR, preventing its self-degradation by blocking the binding of c-Cbl and Grb2. As a result of elevated EGFR levels, CYTOR transcripts are continuously produced (Fig. 7S), indicating an EGFR/AP-1/CYTOR/EGFR feedback amplification loop that operates downstream of ouabain/NKA α1 signaling.

3.8. Ouabain-mediated training effect and immunoparalysis reversal are critically dependent on MORRBID

lncRNAs are poorly conserved in vertebrates. Database analyses have shown that there are no murine lncRNAs that are homologous to the human CYTOR. However, CYTOR exhibits a high degree of similarity to another human lncRNA, miR4435-2HG, with over 99% sequence identity (Supporting Information Fig. S7A). The murine lncRNA MORRBID is a homolog of human miR4435-2HG, which led us to investigate whether MORRBID functions similarly to CYTOR. MORRBID demonstrated an expression pattern similar to that of TNF and IL-1β in the context of LPS-induced tolerance in BMDMs, as shown in Fig. 8A and Fig. S8A-1 and S8A-2. MORRBID expression was unable to be upregulated by a second LPS stimulation in tolerant immune cells (Fig. 8A, Fig. S8B-1 and S8B-2). In BMDMs, MORRBID expression rapidly increased following LPS stimulation but then gradually decreased (Fig. 8B). This pattern mirrored the expression trends of TNF (Fig. S8C-1), IL-1β (Fig. S8C-2), and CYTOR (Fig. 5E). Similar results occurred in other immune cells (Fig. S8D-1 and S8D-2). In tolerant BMDMs, ouabain training significantly upregulated MORRBID expression (Fig. 8C), comparable to its effects on TNF (Fig. S8E-1) and IL-1β (Fig. S8E-2). This upregulation also occurred in other immune

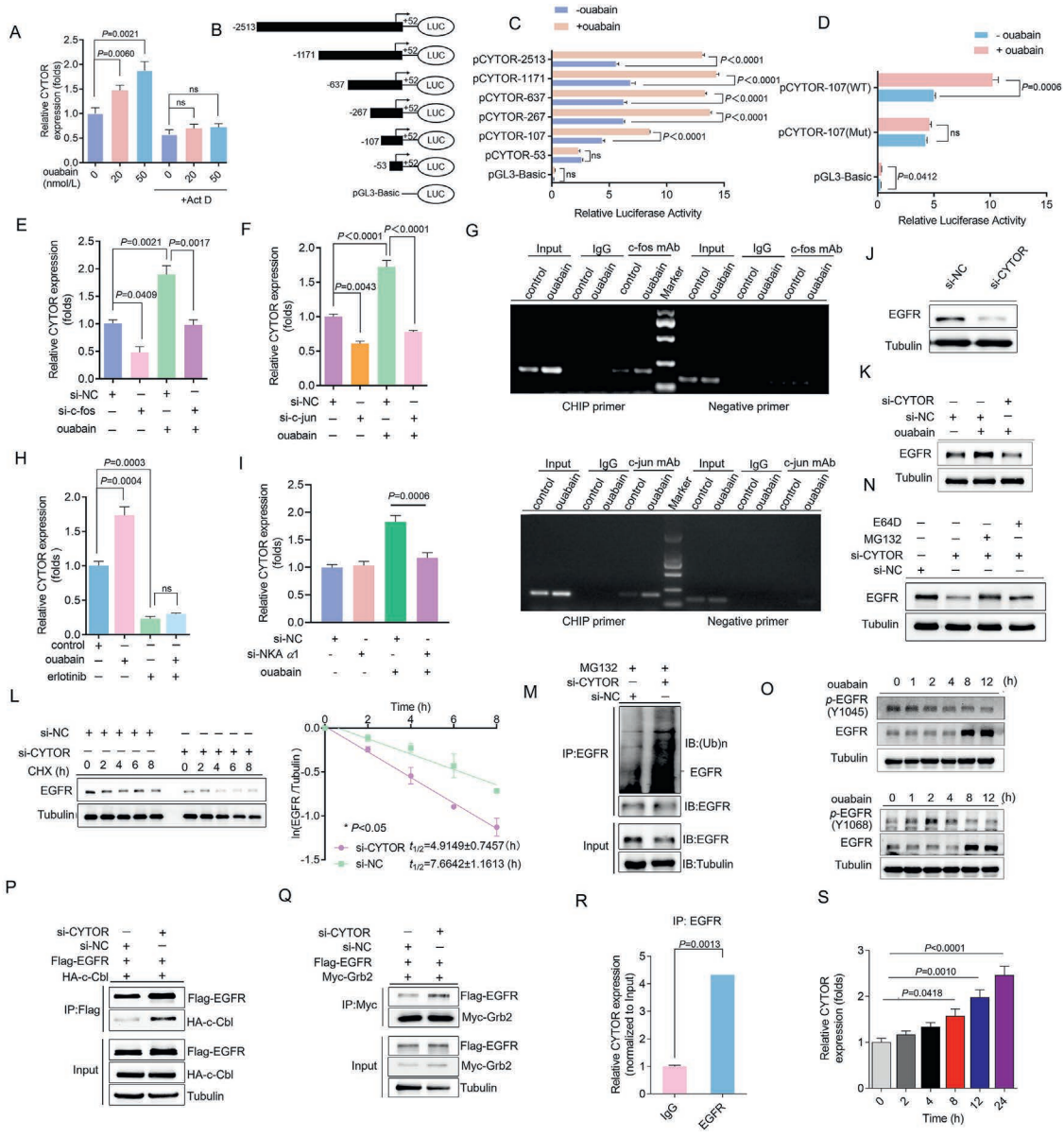

Figure 7 Ouabain increased CYTOR production *via* EGFR/AP-1/CYTOR/EGFR amplification loop. (A) THP1 cells were pre-incubated with Act D (5 μg/mL) and then treated with 20 or 50 nmol/L ouabain for 6 h ($n = 3$). (B) Schematic diagram of CYTOR promoter and its deletion mutants. (C) The HEK293T cells were transfected with a luciferase reporter driven by deletion mutants of the CYTOR promoter. After transfection, the cells were treated with ouabain at 50 nmol/L for 24 h ($n = 3$). (D) The HEK293T cells were transfected with a luciferase reporter driven by the CYTOR promoter (-107 to $+52$) or its variant with mutations in the AP-1 binding sites, then treated with ouabain for 12 h, $n = 3$. THP1 cells were transfected with si-c-Fos (E) or si-c-Jun (F) for 36 h, then treated with or without 50 nmol/L ouabain for 12 h, $n = 3$. (G) THP1 cells were treated with 50 nmol/L ouabain for 12 h, and a ChIP assay was performed to examine the binding of c-Fos and c-Jun on CYTOR promoter, as visualized by RT-PCR analysis using ChIP primers as well as the negative primers. (H) THP1 cells were pre-treated with 20 μmol/L erlotinib for 2 h, then treated with 50 nmol/L ouabain for an additional 12 h, $n = 3$. (I) THP1 cells were transfected with siRNAs targeting NKA α1 for 36 h, then treated with or without 50 nmol/L ouabain for 12 h ($n = 3$). (J) THP1 cells were transfected with si-NC or si-CYTOR for 48 h. (K) THP1 cells were transfected with si-NC or si-CYTOR for 48 h and then further treated with 50 nmol/L ouabain for 12 h. (L) After transfection with siRNAs against CYTOR, THP1 cells were treated with 100 μg/mL CHX for 2, 4, 6, and 8 h, respectively; EGFR protein expression was examined (left), the kinetics of EGFR protein degradation were plotted (right), and the half-life of EGFR degradation was calculated using the formula $\mathrm{Ln}[A]_t = -Kt + \mathrm{Ln}[A]_0$ (right), $n = 3$. (M) EGFR protein level in THP1 cells after CYTOR transfection and treatment with 20 μmol/L MG132 or 20 μmol/L E64D for 6 h. (N) THP1 cells were transfected with siRNA against CYTOR and then treated with 20 μmol/L MG132 for 6 h. EGFR ubiquitination was examined. (O) THP1 cells were treated with 50 nmol/L ouabain at the indicated periods. (P) The HEK293T cells were co-transfected with HA-tagged c-Cbl and Flag-tagged EGFR along with si-NC or si-CYTOR for 48 h, and an anti-Flag IgG was used to immunoprecipitate the EGFR/c-Cbl complex. (Q) HEK293T cells were co-transfected with Myc-tagged Grb2 and Flag-tagged EGFR along with si-NC or si-CYTOR for 48 h, and an anti-Myc IgG was used to immunoprecipitate the EGFR/Grb2 complex. (R) A RIP assay was performed to analyze the interaction between EGFR and the sense strand of CYTOR in THP1 cells, using an anti-EGFR IgG to immunoprecipitate CYTOR ($n = 3$). (S) THP1 cells were treated with ouabain for 0–24 h, and then CYTOR expression was examined ($n = 3$).

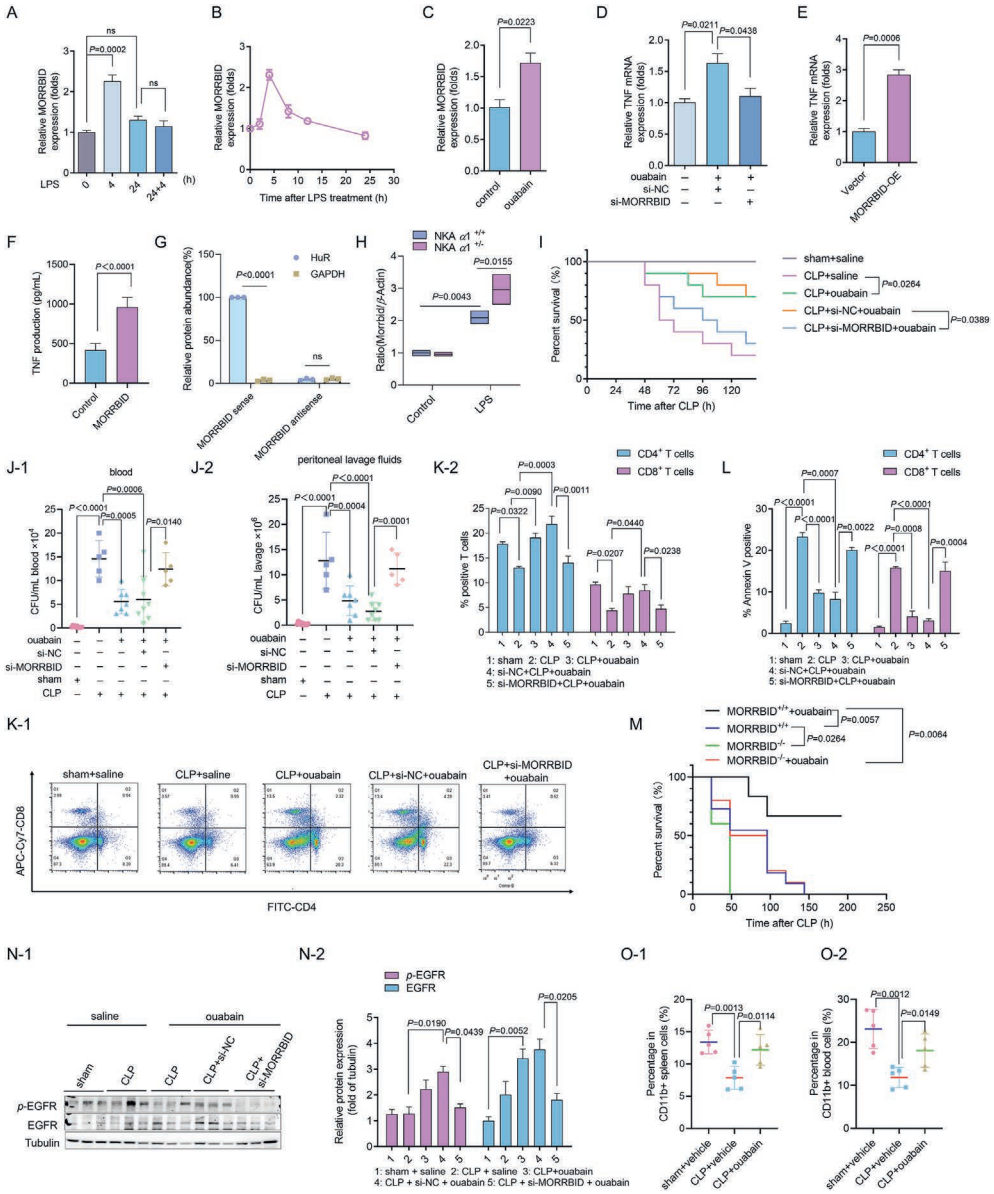

Figure 8 MORRBID is critically involved in the immunoparalysis-reversing effect by ouabain. (A) BMDMs were treated with 1 μg/mL LPS for 4 or 24 h, and the LPS-tolerated cells (24 h) were re-stimulated with LPS for an additional 4 h, $n = 3$. (B) BMDMs were treated with 1 μg/mL LPS for the indicated periods. (C) LPS-tolerized BMDMs were trained with or without 50 nmol/L ouabain ($n = 5$). (D) The LPS-tolerized BMDMs were transfected with siRNAs targeting MORRBID and then treated with ouabain (50 nmol/L) for 8 h ($n = 3$). (E) LPS-tolerized BMDMs were transfected with a MORRBID-expressing plasmid; TNF mRNA expression was examined ($n = 3$). (F) BMDMs were transfected with a MORRBID-expressing plasmid, and then both the control and MORRBID-transfected cells were treated with LPS for 12 h. TNF production was examined ($n = 3$). (G) An RNA pull-down assay detected the interaction between HuR and the sense strand of MORRBID ($n = 3$). (H) PMs from *NKA* $\alpha 1^{+/+}$ or *NKA* $\alpha 1^{+/-}$ mice were treated with LPS (1 μg/mL) for 6 h; MORRBID expression was examined ($n = 3$). (I) CLP mice received saline or ouabain (i.p., 0.1 mg/kg) at 48, 72, 96, and 120 h after CLP; siRNAs against MORRBID were delivered at 48 h before CLP and at 0, 48, and 96 h after CLP, $n = 10$. The bacterial burden in the blood (J-1) and peritoneal lavage fluid (J-2) of CLP mice after ouabain and MORRBID siRNAs treatment was examined, $n = 6$–7. (K-1) Representative flow chart of $CD4^+$ and $CD8^+$ T cell populations in mouse spleens at 96 h after CLP. (K-2) The quantitative results of spleen $CD4^+$ and $CD8^+$ T cells population, $n = 5$. (L) The apoptosis rate of $CD4^+$ and $CD8^+$ T cells in mice spleens at 96 h after CLP, $n = 5$. (M) Mice after macrophage depletion were subjected to CLP surgery at 48 h post-CLP, and mice were adoptively transferred with ouabain-trained BMDMs from $MORRBID^{+/+}$ and $MORRBID^{-/-}$ mice at 48, 72, 96, and 120 h after CLP. *P. aeruginosa* infection was conducted at 72 h post-CLP, $n = 10$. The survival rate of the animals was examined. (N-1) The protein levels of p-EGFR and EGFR in mice spleens at 96 h after CLP. The quantitative result is presented on the right (N-2), $n = 3$. The percentage of $CD11b^+ Ly6C^{hi}Ly6G^{low}$ monocytes in mice spleens (O-1) and blood (O-2) at 96 h after CLP, $n = 5$.

cells (Fig. S8F-1 and S8F-2). Notably, the ouabain-induced increase in TNF (Fig. 8D) and IL-1β (Fig. S8G) expression in tolerant BMDMs was almost completely negated by MORRBID silencing. Much like CYTOR, MORRBID expression independently enhanced TNF expression in tolerant BMDMs (Fig. 8E) and increased the cell's responsiveness to LPS (Fig. 8F). HuR was found to bind to the sense strand of MORRBID (Fig. 8G). CYTOR is known to interact with HuR through loop structures between nucleotides 1-48. Interestingly, identical loop structure sequences were also found in the MORRBID sequences, although the spacer between these two loops differs between CYTOR and MORRBID (Fig. S7B). Furthermore, MORRBID silencing significantly suppressed ouabain's training effect, as indicated by TNF and IL-6 mRNA expression (Fig. S8H1−S8H3). Surprisingly, we found the upregulation of *TNF* and *IL-6* mRNAs by β-glucan training was also significantly suppressed after HuR or MORRBID silencing (Fig. S8I1−S8I3). *NKA α1* knockdown alone failed to increase MORRBID expression, but it can significantly increase LPS-induced MORRBID upregulation (Fig. 8H). Overall, MORRBID closely resembles human CYTOR in terms of its biological functions.

CLP mice were treated with ouabain in combination with methoxy-modified MORRBID siRNAs (Supporting Information Fig. S9A). Ouabain improved animals' survival rates (Fig. 8I), reduced bacterial loads in both blood and peritoneal lavage fluids (Fig. 8J−1 and J-2), and enhanced the production of TNF and IL-1β (Fig. S9B−S9E). However, these beneficial effects were significantly negated by MORRBID silencing (Fig. 8I, J-1, J-2, and Fig. S9B−S9E). Furthermore, ouabain significantly increased spleen $CD4^+$ and $CD8^+$ populations in CLP mice, but this did not occur after MORRBID silencing (Fig. 8K−1 and K-2). Similar trends occurred regarding apoptosis rates in splenic $CD4^+$ and $CD8^+$ T cells (Fig. 8L). To further validate these findings, a significant mortality increase was observed in macrophage-depleted CLP mice transferred with $MORRBID^{-/-}$BMDMs as compared with $MORRBID^{+/+}$BMDMs, and the protective effects of ouabain training were notably diminished in these mice (Fig. 8M). Ouabain also increased the protein levels of EGFR in lung tissues; however, the phosphorylation of EGFR in CLP mice was significantly reduced following MORRBID silencing (Fig. 8N−1 and N-2), indicating that MORRBID may play a role in regulating EGFR signaling and protein expression. A previous study suggested that MORRBID influences the lifespan of monocytes[54]. Correspondingly, the populations of $CD11b^+Ly6^{Chi}Ly6G^{low}$ monocytes in the spleen (Fig. 8O−1) and blood (Fig. 8O−2) of CLP mice were decreased compared to those in the sham control. However, treatment with ouabain significantly increased the monocyte population to nearly 85% of control levels.

3.9. Endogenous ouabain regulates the responsiveness of IICs to endotoxin in vivo

Notably, we observed that PMs from mice treated with anti-ouabain IgG showed reduced responsiveness to LPS compared to those from control IgG-treated mice (Fig. 1O), suggesting that endogenous ouabain (EO) may be present and have a similar effect to that of exogenous ouabain. To confirm this hypothesis, we found that serum levels of EO were present but significantly decreased in CLP mice (Fig. 9A); further, serum levels of EO were well correlated with the responsiveness of macrophages to LPS (Fig. 9B). To further highlight the role of EO, the adrenal glands were removed to create AG^{def} mice, resulting in a significant reduction in EO production[35]. After CLP surgery, PMs from AG^{def} mice exhibited reduced responsiveness to LPS compared to those from intact adrenal gland mice (AG^{int}) (Fig. 9C). Interestingly, exogenous ouabain rescue in AG^{def} CLP mice for 24 h significantly increased macrophage responsiveness to LPS. Consistently, a higher mortality rate was observed in AG^{def} mice compared to the AG^{int} mice after CLP surgery (Fig. 9D). Ouabain treatment, however, significantly improved animal survival, enhanced bacterial clearance in both blood (Fig. 9E) and spleen of AG^{def} mice (Fig. 9F). In contrast, dexamethasone, an adrenal hormone control, did not produce similar beneficial effects. Therefore, ouabain rescue is beneficial for animal survival and bacterial clearance in cases of adrenal gland deficiency. Supporting evidence also shows that survivors of CLP mice had significantly higher serum EO levels compared to non-survivors (Fig. 9G).

EO in human serum is identical to plant ouabain[23,35]. We quantified and compared the serum EO levels in healthy individuals with those patients suffering from sepsis-induced immunoparalysis. As observed in CLP mice, serum EO levels significantly decreased in patients experiencing immunoparalysis (Fig. 9H). The biosynthetic pathway for EO is not fully understood; however, cholesterol is the precursor of EO, and lanosterol synthase (LSS) is a key enzyme involved in EO synthesis[55,56]. A meta-analysis provided by the Biological Information Database of Sepsis (BIDOS) indicated that LSS expression levels were significantly decreased in patients with sepsis, as included in multiple GSE datasheets (Fig. 9I). Similar results were also observed for mevalonate kinase (MVK) (Supporting Information Fig. S10A), another enzyme critically involved in cholesterol synthesis and TRIM[57]. In contrast, IRAK-M, a well-established marker protein of immunoparalysis[33], was significantly upregulated in those patients (Fig. S10B). Notably, serum EO levels in septic patients were positively correlated with TNF production by monocytes in response to LPS (Fig. 9J). TNF production was significantly decreased in patients with immunoparalysis (Figs. 5F and 9J). Accordingly, lower TNF production is associated with poorer survival outcomes in sepsis patients ($n = 239$, Fig. 9K). This further emphasizes TNF's crucial role in regulating immunity during sepsis and the importance of investigating ouabain's effect on TNF expression.

4. Discussion

The steroid hormone ouabain has definite antiseptic properties. Specifically, it can protect against both sepsis-induced hyperinflammation[15] and immunoparalysis models[16]. However, the mechanisms behind these benefits remain unclear. Here, we demonstrate that ouabain, despite brief signaling and rapid metabolic clearance, can induce a significant training effect on peripheral IICs. This effect occurs in tolerant and non-tolerant cells, both *in vitro* and *in vivo*, suggesting it may play a central role in the beneficial effects of ouabain on innate immunity in sepsis. Ouabain's training effect has translational potential because serum levels of EO are significantly reduced in immunoparalysis, correlating with impaired innate immunity. Ouabain-trained IICs can, therefore, be specifically administered during states of immunoparalysis to improve impaired immunity against bacterial infections.

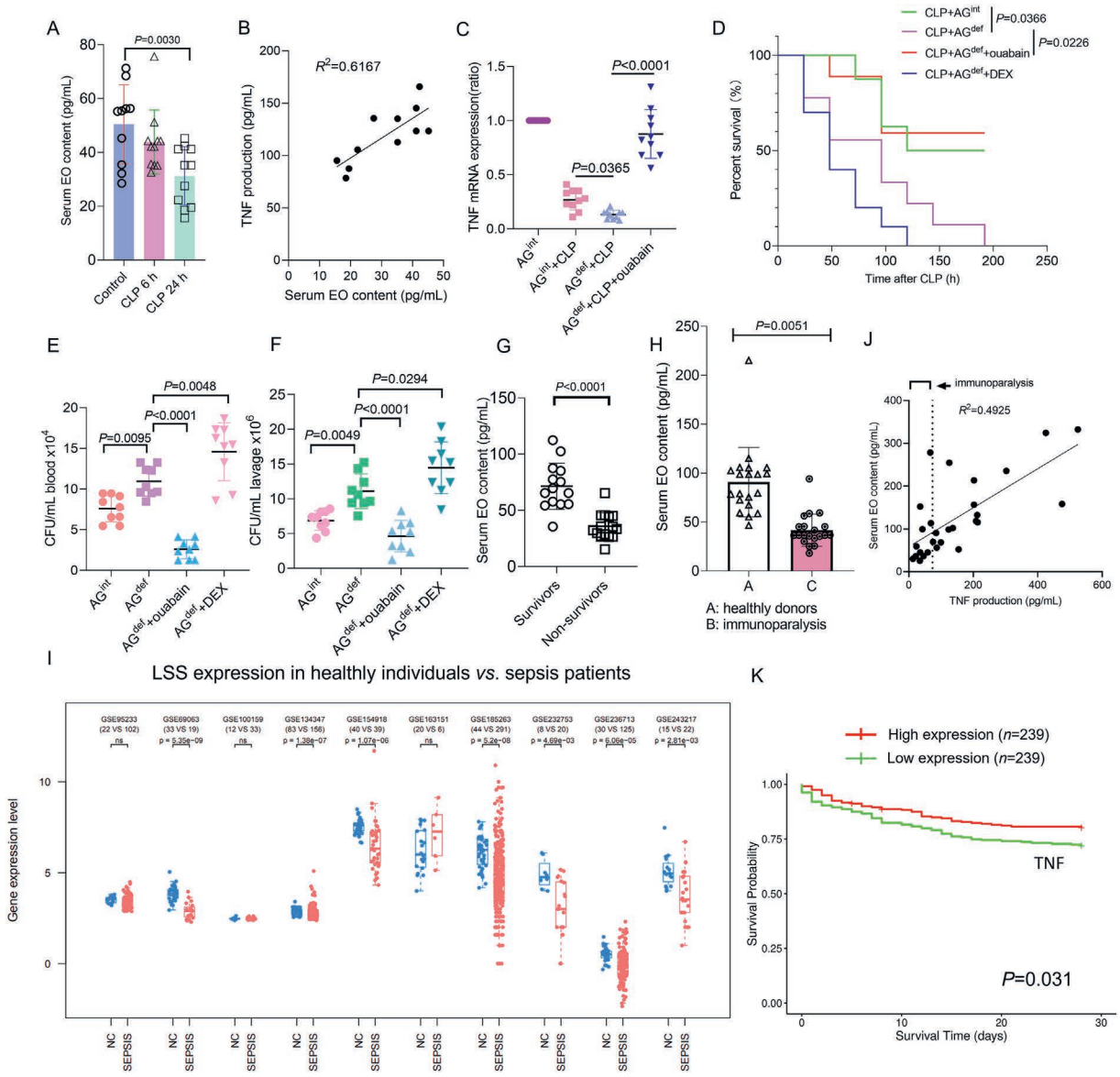

Figure 9 Endogenous ouabain was downregulated in sepsis-induced immunoparalysis. (A) The serum EO contents in CLP mice after surgery for 6 and 24 h, $n = 10-11$. (B) The correlation between serum EO contents and PMs responsiveness to LPS in CLP mice with immunoparalysis. (C) Both AG^{int} and AG^{def} mice were subjected to moderate CLP. AG^{def} CLP mice were further injected with ouabain (0.1 mg/kg, i.p.) for 24 h. PMs from each group were collected, and their responsiveness to LPS was examined ($n = 10$). (D) Groups of AG^{int} and AG^{def} mice were subjected to moderate CLP ($n = 10$). Mice received saline, ouabain, or dexamethasone (DEX, 10 mg/kg, i.g.) at 48, 72, 96, and 120 h after CLP. The bacterial loads in the peritoneal lavage fluid (E) and blood (F) of CLP mice were examined ($n = 9$). (G) The serum EO contents in the survivors and non-survivors of CLP mice, $n = 14-15$. (H) The serum EO contents in healthy individuals and patients with sepsis-induced immunoparalysis, $n = 20$. (I) LSS gene expression in healthy individuals and septic patients, as included in multiple GSE datasheets. (J) Human $CD14^{+}$ monocytes from patients with sepsis and sepsis-induced immunoparalysis were treated with LPS for 8 h, and the correlation between monocyte TNF-producing activity and serum EO content was examined ($n = 28$). (K) Survival probability of septic patients with different expression levels of TNF, $n = 239$. The data are analyzed and provided by the BIODS website (http://www.swmubidos.com/index.php/Index/index).

The training mechanism of ouabain differs from that of β-D-glucan, probably due to its hormonal nature. Ouabain activates an IPRRC to rapidly train mature IICs in the periphery and establish immune memory (Supporting Information Fig. S11). It is important to note that the IPRRC does not refer to a single RNA regulon. Instead, it encompasses a complex and dynamically regulated network that involves multiple interactions among CYTOR, miR181-5p/3p, *TNF* mRNA, HuR, and several signaling molecules, including EGFR, PKCα, and AP-1. CYTOR, but not HuR, plays a central role in the organization and function of the IPRRC. Therefore, this study is distinctly different from prior research, which has only shown HuR's involvement in ouabain-mediated cytokine expression[16]. Without CYTOR, neither HuR nor ouabain can yield a training effect because CYTOR allows

HuR to remain persistently in the cytoplasm, enabling ouabain to have a lasting function-enhancing effect on IICs. All these findings have not been proposed before.

Gene expression at both the epigenetic and posttranscriptional levels is crucial for determining mRNA abundance and protein expression level of a specific gene. However, the role of mRNA reprogramming in the TRIM remains underappreciated. In general, regulating gene expression at the post-transcriptional level is faster and more energy-efficient than regulating it at the transcriptional level, especially during stress conditions when ATP supply is limited[45,58]. In cases of immunoparalysis, as demonstrated in this study, the training mode of ouabain can significantly attenuate the rapid decline in inflammatory cytokines expression in IICs with lower energy expenditure. This approach helps prevent the swift onset and further progression of immune tolerance, thereby maintaining a temporarily controlled immune state that can promote recovery or facilitate subsequent treatment. Therefore, although the training effect of ouabain may not last for months, as seen with Bacillus Calmette-Guérin[59], it can still be effectively used in specific immune and metabolic contexts, such as immunoparalysis, to help restore immune and metabolic balance in a timely and short-acting manner. Additionally, traditional training agents increase lactate production in IICs to meet ATP demand and promote epigenetic rewiring[28,60], however, excess lactate can exacerbate immunosuppression[13]. The Third International Consensus Definitions for Sepsis and Septic Shock (Sepsis-3) has defined serum lactate levels exceeding 2 mmol/L as a clinical criterion for identifying patients with sepsis and septic shock[1]. In addition, the long-lasting effects of training heighten the risk of prolonged inflammatory damage and chronic infections[25]. As such, in the context of sepsis-induced immunoparalysis, ouabain may be beneficial because it has a relatively shorter-lasting and more controllable training effect, in addition to its ability to reduce lactate production. Consistently, in the CLP model, we observed that ouabain has a more beneficial effect on animal survival and bacterial clearance than β-glucan, even when administered at only one percent of β-glucan dosage. More experiments are needed to further support the notion.

Tolerance is an immune state, and training is an immune process; however, they may share overlapping mechanisms[61]. β-glucan can reverse tolerance and induce a training effect through epigenetic reprogramming[28,29]. Here, we propose a model in which ouabain can also reverse tolerance and induce a training effect through mRNA reprogramming, using the expression level of TNF mRNA as a readout of the immune state of IICs (Supporting Information Fig. S12). The balance between gene transcription and mRNA decay determines the level of TNF mRNA in a cell. In tolerant cells, TNF gene transcriptional machinery is shut down. At the same time, TNF mRNA decay is accelerated by microRNAs, such as miR-181d-5p, leading to a failure of TNF production in response to a second LPS stimulation. β-glucan treatment or training can alter the chromosomal state of tolerant IICs through epigenetic reprogramming, thereby reactivating TNF gene transcription machinery and preparing cells for a second LPS stimulation. In contrast, ouabain training induces rapid nuclear export of HuR and facilitates the self-production of CYTOR, which aids in the formation of the CYTOR/HuR complex. It is important to note that the increased CYTOR/HuR complex does not functionally affect TNF production unless the cells undergo a second LPS stimulation, as TNF production remains unchanged during the resting period (Fig. S2D). Moreover, RNA regulons can not only modulate the stability of cytokine mRNA but also regulate their translational efficacy under stressful conditions[46]. As such, we propose that during the resting period of ouabain training, the CYTOR/HuR complex is upregulated to maintain the persistent cytoplasmic retention of HuR, keeping IICs poised for LPS stimulation. When LPS stimulation comes, it rapidly mobilizes the CYTOR/HuR complex to bind to the 3′UTR of target genes, including TNF, IL-6, IL-1β, GM-CSF, and IFN-γ, thereby increasing their mRNA stability and/or translation. The CYTOR/HuR complex induced by ouabain, alongside its associated mRNA reprogramming mechanism, is akin to the enhanced expression of transcription factors and the related epigenetic reprogramming seen in cells trained with β-glucan[62]. Notably, we observed that RNA regulons, including HuR and MORRBID, also play a significant role in the β-glucan-mediated training effect (Fig. 8I). The β-glucan training resulted in a gradual increase in CYTOR production as the duration of the resting period was extended. Additionally, the β-glucan-mediated training effect was significantly inhibited following the silencing of HuR or MORRBID. Therefore, we envision that mRNA reprogramming mediated by IPPRC could be a crucial and general mechanism for TRIM, equally significant as epigenetic reprogramming. This concept requires further evidence for validation.

CYTOR is an important lncRNA linking TRIM and tolerance. Interestingly, while CYTOR can be upregulated by LPS, ouabain, and β-glucan (Figs. 5E and 7T, Fig. S5A), the outcomes of these treatments differ significantly. LPS induces a rapid increase in CYTOR levels, but this is followed by a gradual decline back to baseline. A second LPS stimulus fails to upregulate CYTOR again. Unlike in LPS treatment, the upregulation of CYTOR by ouabain is mediated through an EGFR/AP-1/CYTOR/EGFR self-amplifying circuit. This mechanism permits continuous production of CYTOR, even after ouabain signaling diminishes due to the degradation of NKA α1. In β-glucan-trained cells, CYTOR upregulation occurs less rapidly than that of ouabain, but its expression levels gradually increase as the resting period extends. Additionally, LPS cannot induce HuR nuclear export in tolerant IICs[16]. Ouabain significantly promotes the nuclear export of HuR in tolerant IICs, an effect that β-glucan does not produce. As a result, a second LPS stimulation fails to reverse ET in IICs. The beneficial effects of β-glucan on immunoparalysis reversal *in vivo* are less pronounced than those of ouabain (Fig. 5H and L). Overall, these results suggest that persistent upregulation of CYTOR is essential for effective training and reversing tolerance. However, successful assembly of the CYTOR/HuR complex in the cytoplasm can lead to enhanced TRIM induction and tolerance reversal than CYTOR alone. In support of this notion, we observed in this study that CYTOR not only arrests HuR in the cytoplasm but also anchors HuR onto the 3′-UTR of target mRNAs by acting like a RNA rope, enhancing the interaction between HuR and target mRNAs.

Ligand-induced receptor desensitization is a common mechanism in immune regulation, aiming to prevent the overactivation of signaling pathways[63]. Interestingly, ouabain employs this mechanism to enhance immune training while maintaining metabolic balance, and the reasons are as follows. (1) Prolonged ouabain treatment can result in cell damage and other non-specific side effects. The rapid degradation of the NKA α1 receptor helps to mitigate these undesirable effects. (2) The NKA consumes a significant amount of cellular ATP, and maintaining its function can impose a substantial energy burden, especially during states of immunoparalysis, where metabolic defects are pronounced. The rapid degradation of the NKA α1 helps conserve the limited energy

supply. (3) The NKA α1 is coupled with glycolysis[19,20], but the glycolysis byproduct lactate can aggravate immune suppression[6,13]. Rapid degradation of the NKA α1 helps reduce lactate production. (4) Downregulating NKA α1 expression mimics the effects of ouabain, leading to increased responsiveness of IICs to LPS (Fig. 1C), enhanced nuclear export of HuR (Fig. 3C), and higher expression of MORRBID (Fig. 8H). Therefore, the degradation of NKA α1 is not just a mechanism through which ouabain limits signaling. NKA α1 downregulation assists ouabain in producing a more effective and energy-efficient training effect on IICs.

lncRNAs are important epigenetic regulators of innate immunity[64]. To achieve a relatively durable training effect, ouabain activates CYTOR transcription *via* the *trans*-acting factor AP-1, which is linked to increased chromatin accessibility around the CYTOR gene locus. After transcription, CYTOR forms a complex with EGFR, which amplifies signaling and results in sustained CYTOR transcription. Both EGFR and AP-1 signaling play critical roles in the epigenetic regulation of cytokine production. Therefore, epigenetic reprogramming is indeed partially involved in ouabain's effect. In regulating stress signaling, lncRNAs can be rapidly transcribed with minimal time or energy expenditure, allowing them to bind directly to targeted molecules to perform their functions[65,66]. This characteristic may explain the shorter resting period needed for ouabain to take effect. Furthermore, ouabain reduced lactate production in LPS-induced tolerant cells, likely due to the inhibition of glycolysis mediated by NKA degradation. While ouabain did not alter the total cellular ATP content, it may reduce ATP consumption by NKA, thereby reallocating the limited ATP supply to other processes such as CYTOR transcription or cytokine translation. Additionally, ouabain at low concentrations can promote insulin release and glycogen synthesis[22]. As such, metabolic rewiring may also play a significant role in ouabain's training effect that warrants further investigation.

PKA−cAMP signaling plays a crucial role in β-glucan-induced TRIM by regulating cytokine expression at the epigenetic level[62]. In contrast, Ca^{2+}−PKCα signaling is important for TRIM induction by ouabain, but this regulation occurs at the post-transcriptional level. As such, second messengers are essential upstream regulators of TRIM.

Lower TNF production is linked to poorer survival in septic patients, as shown in this study (Fig. 9K). Analysis of the TNF 3′-UTR sequence reveals an intricate design shaped by natural evolution that supports the regulation of TNF mRNA stability (Fig. 6O). CYTOR acts synergistically with HuR but competes with miR181d-5p for TNF 3′-UTR binding. In LPS-treated cells, miR181d-5p expression was upregulated, while the levels of the CYTOR/HuR complex were decreased. This result led to a rapid decay of TNF mRNA, resulting in heightened immune tolerance. Conversely, in cells trained with ouabain, the CYTOR/HuR complex was upregulated, overriding the effects of miR181d-5p. As a result, *TNF* mRNA stability and expression increased, leading to enhanced function and reversal of tolerance. Interestingly, miR181d-3p, which functions as a "twin" to miR181d-5p, countered the effects of CYTOR. This interaction between miR181d-3p and CYTOR introduces an additional layer of regulation to TNF mRNA stability. The interplay between these intrinsic RNA regulons delicately regulates TNF mRNA stability in a "*Yin*" and "*Yang*" manner; ouabain shifts this balance towards increased TNF mRNA stability by enhancing CYTOR production through a self-amplifying circuit involving CYTOR, EGFR, and AP-1. In summary, this study reveals a previously unknown regulatory mechanism for TNF mRNA stability, which links immune tolerance and TRIM (Supporting Information Fig. S13).

EO and its function executors, CYTOR and MORRBID, were significantly downregulated during immunoparalysis. The rapid decline in TNF expression during immunoparalysis can be attributed to the persistent activation of a complementary anti-inflammatory reaction. EO production is controlled by the hypothalamic-pituitary-adrenal (HPA) axis[18]. This axis is significantly impaired in patients suffering from sepsis[67,68]. Therefore, the downregulation of EO expression during immunoparalysis may result from the failure of the host immune system to restore immune balance (such as restoring TNF expression). Considering this, EO represents a novel factor within the endocrine-immune cross-regulatory network in sepsis.

Ouabain is a clinically prescribed drug for the treatment of heart disease[69]. As a hormone-like substance, ouabain can use NKA as a scaffold protein to initiate signaling events without causing significant toxic effects[15,18]. In this study, we administered a low concentration of ouabain at 0.1 mg/kg *in vivo*, which resulted in a serum ouabain concentration of 115 pg/mL[35], falling within the physiological range of endogenous ouabain (EO) levels. This result suggests that ouabain when utilized at low or physiologically relevant levels, could be repurposed as an immune-regulating agent. Supporting this perspective, ouabain has shown significant antiviral activity[70]. Toad extract (such as Chansu injection in traditional Chinese medicine), which contains several structural analogs of ouabain, has been effectively used in the clinical treatment of infectious diseases, including pharyngitis[71] and COVID-19[72]. It is important to highlight that the mortality rate among patients with cardiac dysfunction and sepsis can reach as high as 90%, necessitating urgent intervention[73]. Ouabain exhibits both cardioprotective and antiseptic effects. Furthermore, ouabain exhibits significant vasopressor activity[15], which may be useful in treating septic shock characterized by both hypotension and elevated lactate levels[1]. Additionally, hyperglycemia is a common characteristic observed in critically ill patients with sepsis[74]; low concentrations of ouabain can stimulate insulin secretion[22]. Taken together, consistent with its defensive role in nature, ouabain may serve as a novel innate immunity regulator in mammals. The non-classical training properties of ouabain demonstrate significant potential in translational medicine for treating sepsis and other infection-related diseases.

5. Limitations of the study

Sepsis involves a complex pathological mechanism, and the immune disorder is just one aspect of it. This research offers preliminary insights into the intricate relationship between ouabain-induced TRIM and immune disorders in sepsis. Further studies are needed to explore the effects of ouabain on other pathological processes related to sepsis. Secondly, this study emphasizes the importance of mRNA reprogramming in the training effect induced by ouabain. However, we cannot rule out the possibility that ouabain may also exert a training effect regulated at the epigenetic or transcriptional level, although this regulatory effect is likely weaker or less significant than that at the post-transcriptional level. Finally, we propose that mRNA reprogramming is a significant mechanism for TRIM. However, this finding may only begin to uncover the complex relationship between mRNA reprogramming and TRIM, as mRNA reprogramming encompasses a broader spectrum of mRNA regulation than what

was observed in this study, including post-transcriptional modifications and translational control, among other factors. Given this, this study just provides an initial glimpse into this fascinating world.

Acknowledgements

This work was supported by the Natural Science Fund of China (82274096, 82373902, 82073916, and 91540119). Key Development Project of Jiangsu Province (BE2023806, China). Scientific Research Program of Shanghai Science and Technology Committee (15411963200, China).

Author contributions

Wu Yin conceived the project, supervised it, and provided financial support. Wu Yin, Lili Chen, Kuida Chen, and RunRun Shan designed the experiments. Lili Chen, Kuida Chen, RunRun Shan, Hao Lin, Jian Liu, Fangzhou Yin, and Wu Yin performed most experiments. Hao Lin aided in data processing. Siyao Zhu aided in microarray and bioinformatics analysis. Yan Chen aided in figures preparation. Wu Yin, Jinjun Bian, and Fangzhou Yin contributed to the discussions. Wu Yin, Lili Chen, Kuida Chen and RunRun Shan prepared the manuscript. PeiPei Jin and Jinjun Bian collected clinical samples. Fangzhou Yin collected clinical samples, performed analysis, and provided partial financial support. All authors have revised and approved the final manuscript.

Conflicts of interest

The authors declare no conflicts of interest.

Appendix A. Supporting information

Supporting information to this article can be found online at https://doi.org/10.1016/j.apsb.2025.12.041.

References

1. Singer M, Deutschman CS, Seymour CW, Shankar-Hari M, Annane D, Bauer M, et al. The third international consensus definitions for sepsis and septic shock (Sepsis-3). *JAMA* 2016;**315**:801−10.
2. Giamarellos-Bourboulis EJ, Aschenbrenner AC, Bauer M, Bock C, Calandra T, Gat-Viks I, et al. The pathophysiology of sepsis and precision-medicine-based immunotherapy. *Nat Immunol* 2024;**25**: 19−28.
3. van der Poll T, Shankar-Hari M, Wiersinga WJ. The immunology of sepsis. *Immunity* 2021;**54**:2450−64.
4. Delano MJ, Ward PA. The immune system's role in sepsis progression, resolution, and long-term outcome. *Immunol Rev* 2016;**274**:330−53.
5. Neves FL, Amaral M, da Silva SFD, Silva IMM, Laranjeira P, Pinto CRJ, et al. Immunoparalysis in critically ill children. *Immunology* 2023;**168**:597−609.
6. Torres LK, Pickkers P, van der Poll T. Sepsis-induced immunosuppression. *Annu Rev Physiol* 2022;**84**:157−81.
7. Lopez-Collazo E, del Fresno C. Pathophysiology of endotoxin tolerance: mechanisms and clinical consequences. *Crit Care* 2013;**17**:242.
8. ber R, Bikker R, Welz B, Christmann M, Brand K. TNF tolerance in monocytes and macrophages: characteristics and molecular mechanisms. *J Immunol Res* 2017;**2017**:9570129.
9. Hotchkiss RS, Monneret G, Payen D. Immunosuppression in sepsis: a novel understanding of the disorder and a new therapeutic approach. *Lancet Infect Dis* 2013;**13**:260−8.
10. Hotchkiss RS, Monneret G, Payen D. Sepsis-induced immunosuppression: from cellular dysfunctions to immunotherapy. *Nat Rev Immunol* 2013;**13**:862−74.
11. Cheng SC, Scicluna BP, Arts RJ, Gresnigt MS, Lachmandas E, Giamarellos-Bourboulis EJ, et al. Broad defects in the energy metabolism of leukocytes underlie immunoparalysis in sepsis. *Nat Immunol* 2016; **17**:406−13.
12. Grondman I, Arts RJW, Koch RM, Leijte GP, Gerretsen J, Bruse N, et al. Frontline science: endotoxin-induced immunotolerance is associated with loss of monocyte metabolic plasticity and reduction of oxidative burst. *J Leukoc Biol* 2019;**106**:11−25.
13. Nolt B, Tu F, Wang X, Ha T, Winter R, Williams DL, et al. Lactate and immunosuppression in sepsis. *Shock* 2018;**49**:120−5.
14. Chaudhuri D, Nei AM, Rochwerg B, Balk RA, Asehnoune K, Cadena R, et al. 2024 focused update: guidelines on use of corticosteroids in sepsis, acute respiratory distress syndrome, and community-acquired pneumonia. *Crit Care Med* 2024;**52**:e219−33.
15. Blaustein MP, Hamlyn JM. Sensational site: the sodium pump ouabain-binding site and its ligands. *Am J Physiol Cell Physiol* 2024; **326**:C1120−77.
16. Dan C, Jinjun B, Zi-Chun H, Lin M, Wei C, Xu Z, et al. Modulation of TNF-alpha mRNA stability by human antigen R and miR181s in sepsis-induced immunoparalysis. *EMBO Mol Med* 2015;**7**:140−57.
17. Matsumori A, Ono K, Nishio R, Igata H, Shioi T, Matsui S, et al. Modulation of cytokine production and protection against lethal endotoxemia by the cardiac glycoside ouabain. *Circulation* 1997;**96**: 1501−6.
18. Bagrov AY, Shapiro JI, Fedorova OV. Endogenous cardiotonic steroids: physiology, pharmacology, and novel therapeutic targets. *Pharmacol Rev* 2009;**61**:9−38.
19. Balaban RS, Bader JP. Studies on the relationship between glycolysis and (Na^+ + K^+)-ATPase in cultured cells. *Biochim Biophys Acta* 1984;**804**:419−26.
20. Meyer DJ, Diaz-Garcia CM, Nathwani N, Rahman M, Yellen G. The Na^+/K^+ pump dominates control of glycolysis in hippocampal dentate granule cells. *eLife* 2022;**11**:e81645.
21. Pierre SV, Yang C, Yuan Z, Seminerio J, Mouas C, Garlid KD, et al. Ouabain triggers preconditioning through activation of the Na^+,K^+-ATPase signaling cascade in rat hearts. *Cardiovasc Res* 2007;**73**: 488−96.
22. Furstenwerth H. Rethinking heart failure. *Cardiol Res* 2012;**3**:243−57.
23. Hamlyn JM, Blaustein MP, Bova S, DuCharme DW, Harris DW, Mandel F, et al. Identification and characterization of a ouabain-like compound from human plasma. *Proc Natl Acad Sci U S A* 1991;**88**: 6259−63.
24. Abaimov DA, Kazanskaya RB, Ageldinov RA, Nesterov MS, Timoshina YA, Platova AI, et al. Evaluation of Ouabain's tissue distribution in C57/Black mice following intraperitoneal injection, using chromatography and mass spectrometry. *Int J Mol Sci* 2024;**25**:4318.
25. Hajishengallis G, Netea MG, Chavakis T. Trained immunity in chronic inflammatory diseases and cancer. *Nat Rev Immunol* 2025;**25**: 497−514.
26. Netea MG, Dominguez-Andres J, Barreiro LB, Chavakis T, Divangahi M, Fuchs E, et al. Defining trained immunity and its role in health and disease. *Nat Rev Immunol* 2020;**20**:375−88.
27. Schrijver DP, Roring RJ, Deckers J, de Dreu A, Toner YC, Prevot G, et al. Resolving sepsis-induced immunoparalysis *via* trained immunity by targeting interleukin-4 to myeloid cells. *Nat Biomed Eng* 2023;**7**: 1097−112.
28. Dominguez-Andres J, Novakovic B, Li Y, Scicluna BP, Gresnigt MS, Arts RJW, et al. The itaconate pathway is a central regulatory node linking innate immune tolerance and trained immunity. *Cell Metab* 2019;**29**:211−220.e5.
29. Novakovic B, Habibi E, Wang SY, Arts RJW, Davar R, Megchelenbrink W, et al. beta-Glucan reverses the epigenetic state of LPS-induced immunological tolerance. *Cell* 2016;**167**:1354−68.e14.
30. Wang JF, Li JB, Zhao YJ, Yi WJ, Bian JJ, Wan XJ, et al. Up-regulation of programmed cell death 1 ligand 1 on neutrophils may be involved

in sepsis-induced immunosuppression: an animal study and a prospective case-control study. *Anesthesiology* 2015;**122**:852−63.
31. Levy MM, Fink MP, Marshall JC, Abraham E, Angus D, Cook D, et al. 2001 SCCM/ESICM/ACCP/ATS/SIS international sepsis definitions conference. *Crit Care Med* 2003;**31**:1250−6.
32. Muenzer JT, Davis CG, Chang K, Schmidt RE, Dunne WM, Coopersmith CM, et al. Characterization and modulation of the immunosuppressive phase of sepsis. *Infect Immun* 2010;**78**:1582−92.
33. Deng JC, Cheng G, Newstead MW, Zeng X, Kobayashi K, Flavell RA, et al. Sepsis-induced suppression of lung innate immunity is mediated by IRAK-M. *J Clin Investig* 2006;**116**:2532−42.
34. Dejager L, Pinheiro I, Dejonckheere E, Libert C. Cecal ligation and puncture: the gold standard model for polymicrobial sepsis?. *Trends Microbiol* 2011;**19**:198−208.
35. Yang K, Li Z, Chen Y, Yin F, Ji X, Zhou J, et al. Na,K-ATPase alpha1 cooperates with its endogenous ligand to reprogram immune microenvironment of lung carcinoma and promotes immune escape. *Sci Adv* 2023;**9**:eade5393.
36. Weisser SB, van Rooijen N, Sly LM. Depletion and reconstitution of macrophages in mice. *J Vis Exp* 2012:4105.
37. Qiu X, Li J, Bonenfant J, Jaroszewski L, Mittal A, Klein W, et al. Dynamic changes in human single-cell transcriptional signatures during fatal sepsis. *J Leukoc Biol* 2021;**110**:1253−68.
38. Li D, Wei R, Zhang X, Gong S, Wan M, Wang F, et al. Gut commensal metabolite rhamnose promotes macrophages phagocytosis by activating SLC12A4 and protects against sepsis in mice. *Acta Pharm Sin B* 2024;**14**:3068−85.
39. Noh JH, Kim KM, Abdelmohsen K, Yoon JH, Panda AC, Munk R, et al. HuR and GRSF1 modulate the nuclear export and mitochondrial localization of the lncRNA RMRP. *Genes Dev* 2016;**30**:1224−39.
40. Zhang W, Pan X, Xu Y, Guo H, Zheng M, Chen X, et al. Mevalonate improves anti-PD-1/PD-L1 efficacy by stabilizing *CD274* mRNA. *Acta Pharm Sin B* 2023;**13**:2585−600.
41. Divangahi M, Aaby P, Khader SA, Barreiro LB, Bekkering S, Chavakis T, et al. Trained immunity, tolerance, priming and differentiation: distinct immunological processes. *Nat Immunol* 2021;**22**:2−6.
42. Bekkering S, Blok BA, Joosten LA, Riksen NP, van Crevel R, Netea MG. *In vitro* experimental model of trained innate immunity in human primary monocytes. *Clin Vaccine Immunol* 2016;**23**:926−33.
43. Liu D, Huang SY, Sun JH, Zhang HC, Cai QL, Gao C, et al. Sepsis-induced immunosuppression: mechanisms, diagnosis and current treatment options. *Mil Med Res* 2022;**9**:56.
44. Schwartz N, Verma A, Bivens CB, Schwartz Z, Boyan BD. Rapid steroid hormone actions *via* membrane receptors. *Biochim Biophys Acta* 2016;**1863**:2289−98.
45. Ivanov P, Anderson P. Post-transcriptional regulatory networks in immunity. *Immunol Rev* 2013;**253**:253−72.
46. Hinman MN, Lou H. Diverse molecular functions of Hu proteins. *Cell Mol Life Sci* 2008;**65**:3168−81.
47. Doller A, Huwiler A, Muller R, Radeke HH, Pfeilschifter J, Eberhardt W. Protein kinase C alpha-dependent phosphorylation of the mRNA-stabilizing factor HuR: implications for posttranscriptional regulation of cyclooxygenase-2. *Mol Biol Cell* 2007;**18**:2137−48.
48. von Knethen A, Tautenhahn A, Link H, Lindemann D, Brune B. Activation-induced depletion of protein kinase C alpha provokes desensitization of monocytes/macrophages in sepsis. *J Immunol* 2005;**174**:4960−5.
49. Chen Y, Li Z, Chen X, Zhang S. Long non-coding RNAs: from disease code to drug role. *Acta Pharm Sin B* 2021;**11**:340−54.
50. van Loo G, Bertrand MJM. Death by TNF: a road to inflammation. *Nat Rev Immunol* 2023;**23**:289−303.
51. Echtenacher B, Urbaschek R, Weigl K, Freudenberg MA, Mannel DN. Treatment of experimental sepsis-induced immunoparalysis with TNF. *Immunobiology* 2003;**208**:381−9.
52. Cui X, Xie Z. Protein interaction and Na/K-ATPase-mediated signal transduction. *Molecules* 2017;**22**:990.
53. Conte A, Sigismund S. Chapter six - the ubiquitin network in the control of EGFR endocytosis and signaling. *Prog Mol Biol Transl Sci* 2016;**141**:225−76.
54. Kotzin JJ, Spencer SP, McCright SJ, Kumar DBU, Collet MA, Mowel WK, et al. The long non-coding RNA Morrbid regulates Bim and short-lived myeloid cell lifespan. *Nature* 2016;**537**:239−43.
55. Iatrino R, Lanzani C, Bignami E, Casamassima N, Citterio L, Meroni R, et al. Lanosterol synthase genetic variants, endogenous ouabain, and both acute and chronic kidney injury. *Am J Kidney Dis* 2019;**73**:504−12.
56. Lanzani C, Citterio L, Glorioso N, Manunta P, Tripodi G, Salvi E, et al. Adducin- and ouabain-related gene variants predict the antihypertensive activity of rostafuroxin, part 2: clinical studies. *Sci Transl Med* 2010;**2**:59ra87.
57. Bekkering S, Arts RJW, Novakovic B, Kourtzelis I, van der Heijden C, Li Y, et al. Metabolic induction of trained immunity through the mevalonate pathway. *Cell* 2018;**172**:135−146.e9.
58. Anderson P. Post-transcriptional regulons coordinate the initiation and resolution of inflammation. *Nat Rev Immunol* 2010;**10**:24−35.
59. Ziogas A, Novakovic B, Ventriglia L, Galang N, Tran KA, Li W, et al. Long-term histone lactylation connects metabolic and epigenetic rewiring in innate immune memory. *Cell* 2025;**188**:2992−3012.e16.
60. Cai H, Chen X, Liu Y, Chen Y, Zhong G, Chen X, et al. Lactate activates trained immunity by fueling the tricarboxylic acid cycle and regulating histone lactylation. *Nat Commun* 2025;**16**:3230.
61. Lopez-Collazo E, Del Fresno C. Endotoxin tolerance and trained immunity: breaking down immunological memory barriers. *Front Immunol* 2024;**15**:1393283.
62. Saeed S, Quintin J, Kerstens HH, Rao NA, Aghajanirefah A, Matarese F, et al. Epigenetic programming of monocyte-to-macrophage differentiation and trained innate immunity. *Science* 2014;**345**:1251086.
63. McKean DJ, Huntoon C, Bell M. Ligand-induced desensitization of interleukin 1 receptor-initiated intracellular signaling events in T helper lymphocytes. *J Exp Med* 1994;**180**:1321−8.
64. Zhang Q, Cao X. Epigenetic regulation of the innate immune response to infection. *Nat Rev Immunol* 2019;**19**:417−32.
65. Chen YG, Satpathy AT, Chang HY. Gene regulation in the immune system by long noncoding RNAs. *Nat Immunol* 2017;**18**:962−72.
66. Bisogno LS, Keene JD. RNA regulons in cancer and inflammation. *Curr Opin Genet Dev* 2018;**48**:97−103.
67. Bornstein SR. Predisposing factors for adrenal insufficiency. *N Engl J Med* 2009;**360**:2328−39.
68. Cooper MS, Stewart PM. Corticosteroid insufficiency in acutely ill patients. *N Engl J Med* 2003;**348**:727−34.
69. Furstenwerth H. Ouabain - the insulin of the heart. *Int J Clin Pract* 2010;**64**:1591−4.
70. Carvalho DCM, da Silva PG, Dantas WM, da Silva SJR, da Silva CTA, Chaves EJF, et al. Antiviral activity of ouabain against a Brazilian Zika virus strain. *Sci Rep* 2022;**12**:12598.
71. Chen KK, Kovarikova A. Pharmacology and toxicology of toad venom. *J Pharmaceut Sci* 1967;**56**:1535−41.
72. Li M, Zhu H, Liu Y, Lu Y, Sun M, Zhang Y, et al. Role of traditional Chinese medicine in treating severe or critical COVID-19: a systematic review of randomized controlled trials and observational studies. *Front Pharmacol* 2022;**13**:926189.
73. Arfaras-Melainis A, Polyzogopoulou E, Triposkiadis F, Xanthopoulos A, Ikonomidis I, Mebazaa A, et al. Heart failure and sepsis: practical recommendations for the optimal management. *Heart Fail Rev* 2020;**25**:183−94.
74. Marik PE, Raghavan M. Stress-hyperglycemia, insulin and immunomodulation in sepsis. *Intensive Care Med* 2004;**30**:748−56.